Reactions of Hydrated Electron with Various Radicals: Spin Factor in Diffusion-Controlled Reactions

Takatoshi Ichino and Richard W. Fessenden*

Radiation Laboratory and Department of Chemistry and Biochemistry, University of Notre Dame, Notre Dame, Indiana 46556-5674

Received: December 8, 2006; In Final Form: January 23, 2007

The reactions of hydrated electron (e_{aq}^-) with various radicals have been studied in pulse radiolysis experiments. These radicals are hydroxyl radical ($^\bullet OH$), sulfite radical anion ($^\bullet SO_3^-$), carbonate radical anion ($CO_3^{\bullet -}$), carbon dioxide radical anion ($^\bullet CO_2^-$), azidyl radical ($^\bullet N_3$), dibromine radical anion ($Br_2^{\bullet -}$), diiodine radical anion ($I_2^{\bullet -}$), 2-hydroxy-2-propyl radical ($^\bullet C(CH_3)_2OH$), 2-hydroxy-2-methyl-1-propyl radical (($^\bullet CH_2)(CH_3)_2$-COH), hydroxycyclohexadienyl radical ($^\bullet C_6H_6OH$), phenoxyl radical ($C_6H_5O^\bullet$), *p*-methylphenoxyl radical (*p*-$(H_3C)C_6H_4O^\bullet$), *p*-benzosemiquinone radical anion (*p*-$OC_6H_4O^{\bullet -}$), and phenylthiyl radical ($C_6H_5S^\bullet$). The kinetics of e_{aq}^- was followed in the presence of the counter radicals in transient optical absorption measurements. The rate constants of the e_{aq}^- reactions with radicals have been determined over a temperature range of 5−75 °C from the kinetic analysis of systems of multiple second-order reactions. The observed high rate constants for all the e_{aq}^- + radical reactions have been analyzed with the Smoluchowski equation. This analysis suggests that many of the e_{aq}^- + radical reactions are diffusion-controlled with a spin factor of $^1/_4$, while other reactions with $^\bullet OH$, $^\bullet N_3$, $Br_2^{\bullet -}$, $I_2^{\bullet -}$, and $C_6H_5S^\bullet$ have spin factors significantly larger than $^1/_4$. Spin dynamics for the e_{aq}^-/radical pairs is discussed to explain the different spin factors. The reactions with $^\bullet OH$, $^\bullet N_3$, $Br_2^{\bullet -}$, and $I_2^{\bullet -}$ have also been found to have apparent activation energies less than that for diffusion control, and it is suggested that the spin factors for these reactions decrease with increasing temperature. Such a decrease in spin factor may reflect a changing competition between spin relaxation/conversion and diffusive escape from the radical pairs.

Introduction

The population of the electron spin states of radicals in solution can transiently deviate from that under thermal equilibrium as a result of spin-selective chemistry and spin dynamics of radical pairs. Such a process is generally known as chemically induced dynamic electron polarization (CIDEP).[1,2] The observation of inverted CIDEP in the reaction of hydrated electron (e_{aq}^-) with phenoxyl radical ($C_6H_5O^\bullet$) and some other radicals has long been a puzzle.[3−6] Two explanations are possible. The initial explanation[3] was that reaction of uncorrelated radical pairs might produce the excited triplet state of the phenolate anion, leaving singlet pairs, and invert the sense of the CIDEP to A/E (ESR absorption at low magnetic field, emission at high field). Subsequent ESR observations of e_{aq}^- and $C_6H_5O^\bullet$ were made in the laser photolysis of phenolate[4] and interpreted as inverted CIDEP for the geminate pairs on the basis that the dissociating state was a singlet. If so, the energy ordering in the radical encounter pairs ($e_{aq}^-/C_6H_5O^\bullet$) must be triplet below singlet. More recently, Bussandri and van Willigen clearly showed that the $e_{aq}^-/C_6H_5O^\bullet$ geminate pair is singlet,[7] suggesting the latter explanation of the inverted CIDEP for this radical pair. In the meantime, Kobori et al. have demonstrated the influence of electronic interaction between the radical ion pair states and the charge-recombined product states on the energy ordering of the radical ion pair states.[8−10] This interaction is closely associated with reorganization energy in electron-transfer theory,[11,12] and we have recently applied this mechanism to a number of radical pairs involving e_{aq}^- to explain their CIDEP patterns.[6]

The present work was originally initiated to see if there is any evidence of a triplet pathway for e_{aq}^- + $C_6H_5O^\bullet$ reaction. The e_{aq}^- is a highly reducing species with a reduction potential of −2.87 V (versus NHE),[13−15] and $C_6H_5O^\bullet$ is an oxidizing radical with a reduction potential of +0.79 V.[16] Thus, the free energy difference for the reaction to form the ground singlet state of phenolate is $\Delta G = -3.66$ eV. Because the energy of the excited triplet state of phenolate is about 3.45 eV,[6] the reaction could form the triplet state. When the reaction took place at a diffusion-controlled rate to form the ground singlet-state product, only $^1/_4$ of the radical pair encounters would be effective[17] and the overall rate constant would reflect that fact. If the product were triplet, then the rate could be three times as fast, or if spin were not important, then product could result from every encounter at four times the rate. This statistical factor will be termed the spin factor in this paper. A careful examination of the rate constants should allow one to distinguish the difference. While apparent success has been achieved in elucidating the mechanism of the inverted CIDEP as described above,[6] such investigation of reactions between e_{aq}^- and $C_6H_5O^\bullet$ or other radicals is desirable in fundamental understanding of radical−radical interactions.

Very little is known about reactions between e_{aq}^- and reactive radicals in general, in stark contrast with a compilation of large kinetics data for e_{aq}^- reactions with nonradical (i.e., stable) compounds.[18,19] Determination of the rate constants of e_{aq}^- +

* Corresponding author. E-mail: fessenden.1@nd.edu.

10.1021/jp0684527 CCC: $37.00
Published on Web 03/13/2007

radical reactions requires an analysis of complex kinetics that results from various first- and second-order reactions, in contrast to a standard analysis of pseudo-first-order kinetics used for e_{aq}^- + nonradical reactions.

The pulse radiolysis of aqueous media generates e_{aq}^-, hydroxyl radical ($^\bullet$OH), hydrogen atom ($^\bullet$H), hydrogen peroxide (H_2O_2), and molecular hydrogen (H_2) as primary species.[20] Thus, e_{aq}^- decays by second-order reactions with these radiolysis products. Among the primary species, the yields of e_{aq}^- and $^\bullet$OH are much larger than those of the others. Therefore, the e_{aq}^- decay is largely influenced by reaction with $^\bullet$OH. The rate constants of the e_{aq}^- + $^\bullet$OH reaction have been determined from the analysis of the e_{aq}^- decay curves in this complex kinetic system.[21−23]

This second-order analysis method is, however, not limited to the study of the e_{aq}^- + $^\bullet$OH reaction. If a solute that is inert to e_{aq}^- but reacts efficiently with $^\bullet$OH is added into the aqueous system, then $^\bullet$OH can be quickly converted to a secondary radical through the reaction with the solute, and the e_{aq}^- decay profile reflects the reaction with the secondary radical. Thus, the second-order analysis of such a system leads to determination of the rate constant of the e_{aq}^- reaction with the secondary radical. Indeed, the e_{aq}^- + $^\bullet$H reaction has been investigated in the radiolysis of an aqueous solution of H_2, where $^\bullet$OH reacts with H_2 to form $^\bullet$H.[21,22] It is possible to study the e_{aq}^- reactions with other radicals by using other hydroxyl scavengers. It should be mentioned that geminate recombination processes for e_{aq}^- following photoionization and photodetachment in aqueous solutions have recently been a subject of experimental studies using ultrafast laser techniques.[24−43] A study of homogeneous kinetics in the systems involving both e_{aq}^- and radicals will certainly help better understand these photoinduced events, as well as radiation-induced events,[44−46] on the fast time scale.

In this report, we present our research on e_{aq}^- reactions with a number of radicals using pulse radiolysis. The radicals studied are $^\bullet$OH, sulfite radical anion ($^\bullet SO_3^-$), carbonate radical anion ($CO_3^{\bullet-}$), carbon dioxide radical anion ($^\bullet CO_2^-$), azidyl radical ($^\bullet N_3$), dibromine radical anion ($Br_2^{\bullet-}$), diiodine radical anion ($I_2^{\bullet-}$), 2-hydroxy-2-propyl radical ($^\bullet C(CH_3)_2OH$), 2-hydroxy-2-methyl-1-propyl radical (($^\bullet CH_2)(CH_3)_2COH$), hydroxycyclohexadienyl radical ($^\bullet C_6H_6OH$), $C_6H_5O^\bullet$, *p*-methylphenoxyl radical (*p*-$(H_3C)C_6H_4O^\bullet$), *p*-benzosemiquinone radical anion (*p*-$OC_6H_4O^{\bullet-}$), and phenylthiyl radical ($C_6H_5S^\bullet$). The rate constants of the e_{aq}^- reactions with the radicals were determined over a temperature range of 5−75 °C. Very high rate constants were found for the e_{aq}^- reactions with all the radicals, and the observed rate constants were analyzed with the Smoluchowski equation. The Smoluchowski equation is often used to evaluate the diffusion-controlled rate constants, k_{diff}.[47]

$$k_{diff} = 4\pi\sigma N_A D R_{eff} \quad (1)$$

Here, σ is the spin factor, N_A is the Avogadro's number, D is the mutual diffusion constant, and R_{eff} is the effective reaction distance,

$$R_{eff} = R_C \cdot [\exp(R_C/R) - 1]^{-1} \quad (2)$$

when both reactants are charged to effect repulsive interaction. The Onsager radius (R_C) is

$$R_C = \frac{Z_A Z_B e^2}{4\pi\epsilon\epsilon_0 k_B T} \quad (3)$$

Also, Z_A and Z_B are the charge numbers for the two reactants, e is the elementary charge, ϵ is the dielectric constant of the medium, ϵ_0 is the vacuum permittivity, k_B is the Boltzmann constant, and T is the temperature.

Usually, the spin factor is assumed to be $^1/_4$ for radical−radical reactions; i.e., only singlet radical pairs react.[17,48−51] However, another value has also been considered. For example, Buxton and Elliot have used a spin factor of $^1/_4$ for the $^\bullet$H + $^\bullet$H reaction but argued for a value of unity for the $^\bullet$OH + $^\bullet$OH reaction where rapid spin relaxation is possible.[52] The present analysis suggests that, while spin factors for e_{aq}^- reactions with some radicals are $^1/_4$, those with other radicals are much larger than $^1/_4$ at room temperature and may change with temperature. These radicals are $^\bullet$OH, $^\bullet N_3$, $Br_2^{\bullet-}$, $I_2^{\bullet-}$, and $C_6H_5S^\bullet$. Large spin factors can be attributed to unique spin dynamics caused by the counter radicals. Detailed discussion will be given about the spin dynamics in these e_{aq}^- reactions.

Experimental Section

Transient optical absorption measurements were carried out with an 8 MeV, Notre Dame LINAC, Titan Beta, TB-8/16-1S.[53] Details of the experimental setup have been given elsewhere.[54] The duration of the electron beam pulses was several nanoseconds. A 1 kW, pulsed high-pressure Xe lamp was used as a probe light source. Light of appropriate wavelength was selected by a monochromator, and cutoff filters were used for observations at longer wavelengths to eliminate the second-order response of the monochromator. A program in the National Instruments LabWindows environment was used to control the experiments and data processing. Typically, time traces of optical absorption from 10 pulse radiolysis events were averaged to achieve a better signal-to-noise ratio.

Highly pure water from an H_2Only system was used for the preparation of sample aqueous solutions. The resistivity of the water was ≥18 MΩ cm, and the total organic content in the water was less than 20 ppb. Sodium borate, potassium hydroxide, potassium iodide, 2-propanol, 2-methyl-2-propanol, and benzene were obtained from Fisher Scientific Co. Potassium thiocyanate, sodium formate, sodium sulfite, *p*-cresol, benzenethiol, and methylviologen dichloride hydrate were from Aldrich Chemical Co. Sodium azide and hydroquinone were from Fluka. Potassium bromide and phenol were from J. T. Baker Chemical Co. Potassium carbonate was from Matheson Co. All the chemicals were used without further purification.

Sample aqueous solutions were typically prepared at pH ∼ 9.2 at room temperature with 0.5 mM sodium borate in 4 L glass bottles. Aqueous solutions of phenols were made to be pH ∼ 11 with potassium hydroxide to have the phenols in their dissociated forms. For the measurements of rate constants of e_{aq}^- reactions with radicals, the aqueous solutions were purged of dissolved oxygen by bubbling with N_2 gas. N_2O gas was used instead for the measurements of the rate constants of radical self-reactions. The sample solutions were drawn through the optical cell with a peristaltic pump on the exit side. The connection between the glass bottle of the sample solution and the optical cell was made with glass tubing with O-ring joints to minimize the permeation of ambient oxygen. Sample solutions flowed continuously throughout the measurements so that every electron beam pulse hit a fresh portion of the solutions. The flow rate was typically 30 cm^3/min and was fast enough to thoroughly flush the cell between radiolysis pulses (a cycle time of about 6 s). The cross-section of the irradiated portion of the cell was typically more than 10 mm in diameter, while the cross-section of the probe light was less than 4 mm in diameter. The optical path length of the cell was 10 mm.

A glass heat exchange unit was inserted before the optical cell to control the temperature of the sample solutions. A mixture of ethylene glycol and water was circulated through the heat exchanger from a constant temperature bath. Bottles of the sample solutions were also immersed in hot or cold baths to help control the temperature. In the case of N_2O-saturated solutions, the sudden heating of the solution inside the heat exchange column resulted in the formation of N_2O gas bubbles that could interfere with the transient optical absorption measurements. To prevent this problem, a bubble trap was inserted between the heat exchanger and the optical cell.[55] This unit was further covered by a chamber filled with N_2 gas, thus contamination of the sample solution by O_2 was minimal. The temperature of the sample solutions was measured with a thermocouple attached to the outer wall of the optical cell. During measurements at a particular temperature, the temperature was steady to ± 0.5 °C.

The dosimetry for pulse radiolysis experiments was carried out with an N_2O-saturated, neutral aqueous solution of 10 mM potassium thiocyanate. The value for the product of the radiation chemical yield of $(SCN)_2^{\bullet -}$, and its optical absorption coefficient ($G\epsilon$) in this system has been reported.[56,57] With a G value of 6.14 (molecules produced per 100 eV of energy absorbed),[58] the absorption coefficient is estimated to be 8300 M^{-1} cm^{-1} at 472 nm.[59] Typical doses in the measurements were in the range from 7 to 22 Gy.

Measurement of the e_{aq}^- concentration and its time dependence was made using the optical absorption at 600 nm. This wavelength was chosen as a compromise between the magnitude of the absorption coefficient and the sensitivity of the detection system (photomultiplier). The optical absorption coefficient of e_{aq}^- has been reexamined recently.[23,60] The absorption peak redshifts as temperature increases.[60,61] The absorption coefficient at its peak wavelength has been determined as a function of temperature.[23] The absorption coefficient at 600 nm was determined by taking the ratio of absorbances at the peak wavelength and 600 nm at each temperature. The absorption coefficient so determined and that estimated from the thiocyanate dosimetry were in good agreement to within 5%.

A few laser photolysis experiments were performed on cresolate and hydroquinone dianion to analyze the $e_{aq}^- +$ radical reaction rates at various temperatures in a fashion similar to the radiolysis experiments. A flat optical cell with 2 mm inner spacing and an excimer laser at 308 nm were used in these experiments. Transient optical absorption spectra were recorded for an Ar-saturated aqueous solution of 6×10^{-4} M *p*-cresol at pH 13 and an N_2-saturated aqueous solution of 3×10^{-4} M hydroquinone dianion at pH 13. The transient spectra could be accurately fit by equimolar contributions from the absorption spectra of e_{aq}^- and *p*-$(H_3C)C_6H_4O^\bullet$ or *p*-$OC_6H_4O^{\bullet -}$.

Results and Discussion

Reaction of e_{aq}^- with Hydroxyl Radical. Transient optical absorption measurements were first conducted to test how the method of kinetic analysis for the e_{aq}^- reaction with $^\bullet$OH worked in our hands. Very careful attention to the experimental details (particularly the avoidance of impurities) is necessary in this work. Figure 1 shows the time profiles of the optical absorption at 600 nm in the pulse radiolysis of N_2-saturated, borate-buffered water at 7.9 and 22 Gy for both 20 and 72 °C. The distinct time profiles at the two dose levels clearly indicate that e_{aq}^- decays mainly by second-order processes.

Kinetic analysis was performed in order to determine the rate constant of the $e_{aq}^- + {}^\bullet$OH reaction. The kinetic model for the reactions of the radiation chemical species in pure water involves 10 reactions important for e_{aq}^- decay processes.[22,23] Table 1 lists the yields of the species, representing the yields after the completion of the inhomogeneous spur reactions at about 100 ns after the radiolysis pulse.[62] Table 2 gives the rate constants at 298 K and apparent activation energies[63] for the 10 reactions. The apparent activation energies have been calculated for the rate constants over a temperature range from room temperature to about 75 °C. Some of the reactions shown in Table 2 have been studied above 100 °C, and the apparent activation energies tend to decrease at higher temperatures. The e_{aq}^- reaction with proton, another radiolysis product, is not listed in Table 2. The system is basic (pH $\sim$ 9) such that this reaction is negligible.

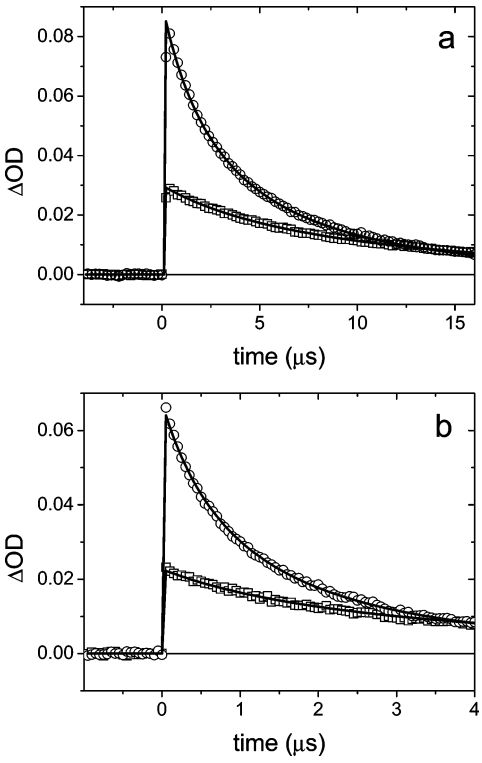

Figure 1. Time profiles of the optical absorption at 600 nm in the pulse radiolysis of N_2-saturated, borate-buffered water at 7.9 Gy (□) and 22 Gy (○) at 20 °C (a) and 72 °C (b). The solid lines are the fitted curves. Note the different time scales.

TABLE 1: Temperature Dependence of *G* Values for Primary Species in Water Radiolysis[a]

primary species	*G* value (molecules/100 eV)
e_{aq}^-	$2.56 + (3.40 \times 10^{-3})T$
$^\bullet$OH	$2.64 + (7.17 \times 10^{-3})T$
$^\bullet$H	$0.54 + (1.28 \times 10^{-3})T$
H_2	$0.43 + (0.69 \times 10^{-3})T$
H_2O_2	$0.72 - (1.49 \times 10^{-3})T$

[a] From ref 62. T is in units of °C.

Curve fitting of the transient optical absorption of e_{aq}^- was implemented with numerical integration of a set of differential equations representing the reactions in the system (Table 2). The Marquardt algorithm was adopted[64] to carry out nonlinear least-square fitting simultaneously for two time profiles at different dose levels at each temperature. Usually, the portion of decay curves between $\sim$1 and 4 to 10 μs after the electron beam pulse was used for the fitting processes. Besides the data provided in Tables 1 and 2, the temperature dependence of pK_w of water[65] and pK_a of borate buffer[66] was taken into account in the kinetic model. It was found that better fits to the data were obtained when a first-order decay constant for e_{aq}^- was added

TABLE 2: Rate Constants and Apparent Activation Energies for Reactions of Primary Species in Water Radiolysis

reaction	k (M^{-1} s^{-1}) at 298 K	E_{app} (kJ mol^{-1})
$e_{aq}^- + e_{aq}^- \rightarrow H_2$[a]	6.4×10^9	20.3
$^\bullet OH + {}^\bullet OH \rightarrow H_2O_2$[b]	4.6×10^9	9.6
$e_{aq}^- + H_2O_2 \rightarrow {}^\bullet OH + OH^-$[c]	1.3×10^{10}	12.4
$e_{aq}^- + {}^\bullet H \rightarrow H_2$[d]	2.6×10^{10}	14.0
$^\bullet H + {}^\bullet OH \rightarrow H_2O$[b]	1.6×10^{10}	9.1
$^\bullet OH + H_2O_2 \rightarrow {}^\bullet O_2H + H_2O$[e]	3.0×10^7	14.0
$^\bullet OH + H_2 \rightarrow {}^\bullet H + H_2O$[f]	3.9×10^7	19.0
$^\bullet H + {}^\bullet H \rightarrow H_2$[g]	5.5×10^9	14.7
$^\bullet H + OH^- \rightarrow e_{aq}^- + H_2O$[h]	2.4×10^7	38.4
$^\bullet H + H_2O_2 \rightarrow {}^\bullet OH + H_2O$[i]	3.6×10^7	21.1

[a] Refs 23 and 60. The apparent activation energy was derived from the rate constants in the temperature range of 20−150 °C. [b] Ref 52. The apparent activation energy was calculated from the observed rate constants over the temperature range of 20−80 °C. [c] Ref 93. [d] Ref 22. [e] Ref 164. [f] Ref 165. [g] Ref 166. [h] Ref 167. [i] Ref 168.

TABLE 3: Optimum Values for Kinetic Parameters in Radiolysis of Pure Water

T (°C)	k_{obs} ($e_{aq}^- + {}^\bullet OH$) (M^{-1} s^{-1})[a]	k_{obs} (first-order) (s^{-1})	σR (Å)[b]	R (Å) with $\sigma = 1/4$[c]
8.7	2.37×10^{10}	5.15×10^3	7.19	28.8
20.2	2.98×10^{10}	1.63×10^4	6.37	25.5
33.5	3.86×10^{10}	1.29×10^4	5.85	23.4
46.4	4.65×10^{10}	4.72×10^3	5.13	20.5
57.1	6.21×10^{10}	1.05×10^4	5.40	21.6
71.8	8.07×10^{10}	8.69×10^3	5.17	20.7

[a] The second-order rate constants have statistical errors of ±10%. [b] Product of the spin factor and the reaction distance for the cross-radical reaction estimated from the Smoluchowski equation. [c] Reaction distance in the case of a spin factor of 1/4.

as another fitting parameter to account for e_{aq}^- reactions with any impurities. The rate constant for $e_{aq}^- + {}^\bullet OH$ and the first-order rate constant for e_{aq}^- decay were so determined. The results of the curve fitting are shown in Figure 1 as solid lines. The fit to the data is excellent. Table 3 lists the rate constants for the e_{aq}^- reaction with $^\bullet OH$ as well as the first-order decay constants.

Elliot and Ouellette[23] and Christensen et al.[22] have independently investigated the $e_{aq}^- + {}^\bullet OH$ reaction in the pulse radiolysis of pure water. The rate constant at room temperature determined in the present study is in good agreement with those from the two groups. On the other hand, our rate constant at higher temperature (8.0×10^{10} M^{-1} s^{-1} at 71 °C) is very close to that from Christensen et al. (8.1×10^{10} M^{-1} s^{-1} at 75 °C) while it differs considerably from that determined by Elliot and Ouellette (5.0×10^{10} M^{-1} s^{-1} at 75 °C). The reason for this discrepancy is not clear. Christensen et al. used silicate buffer (~10 mM) instead of borate buffer used in this study (~0.5 mM) and by Elliot and Ouellette (~1 mM). Although the silicate buffer sets the pH of the system slightly higher than that for the borate system, the difference should have no significant effect on the kinetic behavior. A relatively high concentration of silicate in the work of Christensen et al. might have resulted in more e_{aq}^- decay due to reactions with impurities. On the other hand, they used relatively high dose levels from 16 to 58 Gy so that any first-order reactions were relatively less important (see below). Elliot and Ouellette used dose levels comparable to ours. They conducted kinetic analysis with two fitting parameters including a first-order term as in our study. On the other hand, Christensen et al. did not consider a first-order decay term, which may be reasonable in light of the relatively high doses used in their experiments. However, if the e_{aq}^- first-order decay were significant, then their rate constant for the $e_{aq}^- + {}^\bullet OH$ reaction would have been lower than reported and closer to that of Elliot and Ouellette. Neither of the two groups employed a statistical method such as the Marquardt algorithm for the optimization of the fitting parameters. We note that the value of the first-order rate constant determined in the current work (~1×10^4 s^{-1} at 20 °C) is quite similar to that of Elliot and Ouellette. Both Elliot and Ouellette and Christensen et al. used high-pressure systems (~10 MPa) to extend their study to above 100 °C. This condition is not expected to change the kinetic behavior, and Christensen et al. demonstrated that the rate constants determined at 10 MPa were equal to those determined at 1 atm.

The source of the e_{aq}^- first-order decay is not clear. Reaction with residual oxygen (O_2) is always a possibility. However, careful measures were taken to remove it from our solutions, and it is doubtful that O_2 was present at a very significant concentration. The O_2 concentration in our experimental system was checked by transient optical absorption measurements in the pulse radiolysis of an N_2-saturated aqueous solution of methylviologen (MV^{2+}) and sodium formate.[67] The analysis led to the conclusion that the O_2 concentration was much less than 1 μM. The pseudo-first-order rate constant for the $e_{aq}^- + O_2$ reaction, therefore, is less than the value found, ~1×10^4 s^{-1}. Another possibility is impurities from the borate buffer. However, the high purity of borate used in our measurements is against this possibility, especially when the borate concentration was not high (0.5 mM). It should also be remembered that the purity of the water was also very good.

Because the origin of the e_{aq}^- first-order decay is not clear, a question arises as to whether it is valid to include the corresponding rate constant as a fitting parameter in the analysis. The effect of this parameter on the analysis was assessed by determining the fraction of the e_{aq}^- decay by the first-order process over the time interval used in the analysis. The contribution was typically <5% at the higher dose and <10% at the lower dose of the overall e_{aq}^- decay. Thus, the presence of the first-order decay term in our analysis does not greatly affect the outcome of the optimization of the rate constant for the $e_{aq}^- + {}^\bullet OH$ reaction. The fit of the calculated curves to the data is significantly improved when the first-order reaction is included.

Reactions of e_{aq}^- with Secondary Radicals. With a relatively high concentration of an $^\bullet OH$ scavenger, radiolytically produced $^\bullet OH$ will be rapidly converted into a secondary radical. Thus, the rate constants of the e_{aq}^- reaction with the secondary radical can be determined from the analysis of the e_{aq}^- decay kinetics. The scavenger must have a high rate constant with $^\bullet OH$ but must not react efficiently with e_{aq}^-. Table 4 lists the $^\bullet OH$ scavengers used in our study together with corresponding secondary radicals. The analysis method is basically identical with that for the experiments on pure water, but additional factors must be taken into account. These include the reactions of $^\bullet OH$ as well as $^\bullet H$ with the scavengers, the self-reactions of the secondary radicals, and any optical absorption by the secondary radicals. Details involved in these additional considerations are provided in the Supporting Information, and only the parameters essential for the kinetic analysis are given here. The rate constants of the $^\bullet OH$ and $^\bullet H$ reactions with the scavengers at 298 K and apparent activation energies[63] are given in Table 4. The analogous information on the self-reactions of the secondary radicals, obtained from our experiments, is shown in Table 5.

Transient optical absorption measurements were conducted in the pulse radiolysis of N_2-saturated, borate-buffered aqueous

TABLE 4: Rate Constants and Apparent Activation Energies for Hydroxyl Radical and Hydrogen Atom Reactions with Scavengers

scavenger (S)/secondary radical	k (•OH + S) (M^{-1} s^{-1}) at 298 K; E_{app} (kJ mol^{-1})[a]	k (•H + S) (M^{-1} s^{-1}) at 298 K; E_{app} (kJ mol^{-1})[a]
$(CH_3)_2CHOH/•C(CH_3)_2OH$	2.3×10^9; 5[b]	1.0×10^8; 22.0[c]
$(CH_3)_3COH/(•CH_2)(CH_3)_2COH$	6.3×10^8; 10[b]	
$HCO_2^-/•CO_2^-$	3.6×10^9; 8.5[b]	2.1×10^8[d]
$SO_3^{2-}/•SO_3^-$	5.1×10^9[e]	
$CO_3^{2-}/CO_3•^-$	4.0×10^8; 23.6[f]	
$C_6H_6/•C_6H_6OH$	7.8×10^9; 10[g]	1.1×10^9; 19.1[h]
Br^- / $Br_2•^-$	*i*	*j*
$I^-/I_2•^-$	*i*	*j*
$N_3^-/•N_3$	1.2×10^9[k]	1.9×10^9[l]
$C_6H_5O^-/C_6H_5O•$	4.3×10^9[m]	*n*
p-$(H_3C)C_6H_4O^-$ / *p*-$(H_3C)C_6H_4O•$	4.3×10^9[m]	*n*
p-$^-OC_6H_4O^-$/*p*-$OC_6H_4O•^-$	4.5×10^9[m]	*n*
$C_6H_5S^-/C_6H_5S•$	4.3×10^9[m]	*n*

[a] An activation energy of 10 kJ mol^{-1} was assumed for reactions whose activation energies have not been reported. [b] Ref 169. [c] Ref 170. [d] Ref 18. [e] Ref 171. [f] Ref 172. In our experiment, CO_3^{2-} was in equilibrium with HCO_3^-. The •OH reaction with HCO_3^- was also taken into account in our analysis. [g] Ref 173. The apparent activation energy was estimated over a temperature range of 20−70 °C. [h] Ref 174. [i] The •OH reactions with the halide anions lead to formation of the dihalogen radical anions in multiple steps. See Supporting Information. [j] The •H reactions with the halide anions were neglected in our analysis. See Supporting Information. [k] Ref 175. [l] Ref 176. [m] The rate constants represent the reactions of $•N_3$ with the phenolate anions. For *p*-$(H_3C)C_6H_4O^-$ and $C_6H_5S^-$, the rate constants were assumed to be identical with that for $C_6H_5O^-$ (ref 175). The rate constants for the reactions of $Br_2•^-$ with the phenolate anions are also available (ref 177). [n] In the system of $•N_3$ as an oxidant, •H reacted with N_3^- preferably. In the system of $Br_2•^-$ as an oxidant, •H reactions with the phenolate anions were taken into account. These reactions were treated as the •H reaction with C_6H_6.

TABLE 5: Rate Constants and Apparent Activation Energies for Self-Reactions of Secondary Radicals

radical	$2k_{obs}$ (M^{-1} s^{-1}) at 298 K[a]	E_{app} (kJ mol^{-1})
$•C(CH_3)_2OH$	1.4×10^9	13.9 ± 0.9
$(•CH_2)(CH_3)_2COH$	1.2×10^9	12.0 ± 0.5
$•CO_2^-$	1.0×10^9	8.24 ± 0.67
$•SO_3^-$	1.0×10^9	10.6 ± 0.7
$•C_6H_6OH$	1.5×10^9	20.8 ± 1.5
$Br_2•^-$	4.3×10^9	9.78 ± 0.47
$I_2•^-$	6.4×10^9	14.3 ± 0.9
$•N_3$	7.8×10^9	15.0 ± 0.4
$C_6H_5O•$	2.6×10^9[b]	18.4[c]
p-$(H_3C)C_6H_4O•$	1.7×10^9	18.4 ± 0.8
$C_6H_5S•$	6.1×10^9	17.6 ± 1.1

[a] The second-order rate constants have statistical errors of ±10%. [b] Value from ref 94. [c] Assumed to be the same as for *p*-$(H_3C)C_6H_4O•$.

solutions of hydroxyl scavengers (1−10 mM). A more alkaline condition (pH ∼ 11) was established for the phenol systems to ensure that the phenols were in their dissociated forms, while the carbonate system served as its own buffer (pK_a 10.3).[65] Figure 2 displays the time profiles of the optical absorption at 600 nm in the pulse radiolysis of an N_2-saturated, borate-buffered aqueous solution of 10 mM 2-propanol at 21 and 73 °C together with fitted curves. The rate constant of the e_{aq}^- + $•C(CH_3)_2OH$ reaction was found to be 4.9×10^9 M^{-1} s^{-1} at 21 °C. This rate constant is much smaller than that for the e_{aq}^- + •OH reaction at room temperature. Figure 3 compares the e_{aq}^- decay in N_2-saturated, borate-buffered water alone with that also containing 10 mM 2-propanol, both at 7.9 Gy of radiolysis at room temperature. The difference in the rate constants of the

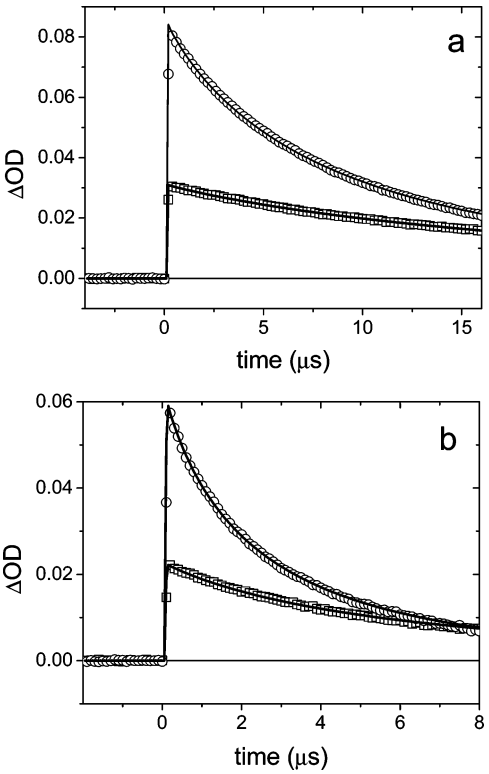

Figure 2. Time profiles of the optical absorption at 600 nm in the pulse radiolysis of an N_2-saturated, borate-buffered aqueous solution of 10 mM 2-propanol at 8.0 Gy (□) and 22 Gy (○) at 21 °C (a) and 73 °C (b). The solid lines are the fitted curves. Note the different time scales.

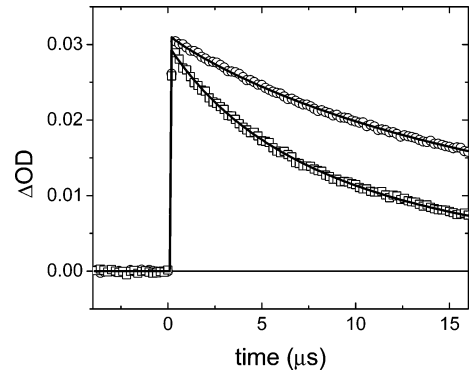

Figure 3. Comparison of the e_{aq}^- decay curves in the pulse radiolysis of N_2-saturated, borate-buffered water (□) and an N_2-saturated, borate-buffered aqueous solution of 10 mM 2-propanol (○) at the same dose level (8 Gy) at room temperature.

e_{aq}^- reactions in the two cases is evident in the slower decay in the 2-propanol system, where •OH is replaced by $•C(CH_3)_2OH$. Table S3 in Supporting Information gives, for the various temperatures, the rate constants for the e_{aq}^- reactions with all the secondary radicals as well as the e_{aq}^- first-order decay constants.

Comments on the first-order decay terms are in order. With relatively high concentrations of scavengers, the concentrations of impurities are inevitably higher in the scavenger systems than in pure water. Thus, there is more chance for e_{aq}^- reactions with impurities. Another point is that some •OH scavengers have moderate reactivity with e_{aq}^-. For instance, e_{aq}^- reacts with benzene (C_6H_6) with a rate constant of 1.0×10^7 M^{-1} s^{-1} at room temperature.[68] Thus, in an aqueous solution of 1 mM C_6H_6, the e_{aq}^- reaction with C_6H_6 leads to a pseudo-first-order decay with a rate constant of 1.0×10^4 s^{-1} at room temperature. This

TABLE 6: Diffusion Constants, Radii, and Spin Relaxation Times of Radicals at 298 K

radical	D (m^2 s^{-1})	R (Å)	T (s)
e_{aq}^-	4.9×10^{-9}[a]	2.5[l]	8×10^{-6}[w]
$^{\bullet}OH$	2.1×10^{-9}[b]	1.7[m]	$<1 \times 10^{-9}$[x]
$^{\bullet}C(CH_3)_2OH$	1.0×10^{-9}[c]	2.8[n]	2.7×10^{-6}[y]
$(^{\bullet}CH_2)(CH_3)_2COH$	8.8×10^{-10}[c]	2.9[o]	$\sim 1 \times 10^{-6}$[z]
$^{\bullet}CO_2^-$	1.7×10^{-9}[d]	1.7[p]	$\sim 1 \times 10^{-8}$[z]
$^{\bullet}SO_3^-$	1.3×10^{-9}[e]	2.6[q]	2.0×10^{-6}[y]
$CO_3^{\bullet -}$	1.2×10^{-9}[f]	1.6[r]	$\sim 1 \times 10^{-8}$[z]
$^{\bullet}C_6H_6OH$	1.1×10^{-9}[g]	3.1[s]	$\sim 1 \times 10^{-6}$[z]
$Br_2^{\bullet -}$	1.6×10^{-9}[h]	2.2[t]	
$I_2^{\bullet -}$	1.6×10^{-9}[h]	2.4[t]	
$^{\bullet}N_3$	1.8×10^{-9}[i]	2.0[u]	
$C_6H_5O^{\bullet}$	1.1×10^{-9}[g]	3.0[v]	$\sim 1 \times 10^{-6}$[z]
p-$(H_3C)C_6H_4O^{\bullet}$	9.2×10^{-10}[j]	3.1[v]	$\sim 1 \times 10^{-6}$[z]
p-$OC_6H_4O^{\bullet -}$	9.5×10^{-10}[k]	3.1[v]	2.0×10^{-6}[aa]
$C_6H_5S^{\bullet}$	1.1×10^{-9}[g]	3.1[v]	

[a] Refs 70 and 71. [b] Ref 72. [c] The diffusion constants of the parent alcohols (refs 178 and 179). [d] Ref 69. [e] The diffusion constant of SO_3^{2-} (ref 180). [f] The diffusion constant of HCO_3^- (ref 180). [g] The diffusion constant of C_6H_6 (refs 181 and 182). [h] The average of the diffusion constants of the corresponding halide anion and trihalide anion (ref 183). [i] The diffusion constant of N_3^- (ref 180). [j] The diffusion constant of $C_6H_5(CH_3)$ (refs 182 and 184). [k] The diffusion constant of OC_6H_4O (ref 185). [l] The radius was estimated from the solvation structure (ref 186). [m] The radius was estimated for H_2O molecule from the density (ref 180). [n] The radius was estimated for $(CH_3)_2CHOH$ from the molar volume in aqueous solution (ref 187). [o] The radius was estimated for $(CH_3)_3COH$ from the molar volume of $(CH_3)_2CHOH$ in aqueous solution (ref 187) and an additional contribution of the CH_3 group (refs 188 and 189). [p] The radius was estimated for HCO_2^- from the hydration enthalpy (ref 190). [q] The radius was estimated for SO_3^{2-} from the hydration enthalpy (ref 190). [r] The radius was estimated for HCO_3^- from the hydration enthalpy (ref 190). [s] The radius was estimated for cyclohexanol from the density of the pure liquid (ref 180). [t] The radius was estimated for the corresponding dihalogen from the crystallographic data (ref 191). [u] The radius was estimated for N_3^- from the hydration enthalpy (ref 190). [v] The radius was estimated for from the molar volume of C_6H_6 in aqueous solution (ref 192) and an additional contribution from the corresponding substitution group (refs 188 and 189). [w] Ref 193. [x] Ref 78. [y] Ref 194. [z] The relaxation time was estimated from the ESR line width (refs 76, 97−99, and 195−198). [aa] Ref 144.

value is consistent with the first-order rate constant determined from the analysis in the benzene system (see Supporting Information). This finding may indicate the ability of our analysis to discriminate between second-order and first-order decays. Also, the first-order rate constants in the solutions of phenolate, *p*-cresolate, hydroquinone dianion, and benzenethiolate are likely to reflect the reactions of e_{aq}^- with the solutes.

Analysis with the Smoluchowski Equation. The e_{aq}^- reactions with all the radicals have large rate constants (see Supporting Information), and it seems probable that these reactions are diffusion controlled. An attempt is made in this section to analyze the rate constants at room temperature with the Smoluchowski equation. The temperature dependence of the rate constants will be considered in the next section. The physical parameters involved in the Smoluchowski analysis, i.e., mutual diffusion constants, reaction distances, and spin factors, are discussed below.

Usually, radical−radical reactions are assumed to take place to form singlet products. Under this assumption, the spin factor in the Smoluchowski equation (eq 1) should be $^1/_4$.[17] For the initial analysis, a spin factor of $^1/_4$ will be used, but this question will be examined in depth later.

The mutual diffusion constants (i.e., the summation of the diffusion constants of the two reactants) can be evaluated rather precisely for our e_{aq}^- + radical systems. The diffusion constants of e_{aq}^- and $^{\bullet}CO_2^-$ have been determined to be 4.9×10^{-9} and 1.7×10^{-9} m^2 s^{-1}, respectively, at room temperature from the conductivity measurements in pulse radiolysis experiments.[69−71] Polarographic measurements have been conducted to determine the diffusion constant of $^{\bullet}OH$ to be 2.0×10^{-9} m^2 s^{-1} at room temperature in pulse radiolysis experiments.[72] The diffusion constants of the other radicals have never been reported. Therefore, their diffusion constants were estimated from those of molecules of similar size and structure, as listed in Table 6. Because the diffusion constant for e_{aq}^- at room temperature will dominate in determining the mutual diffusion constants, the latter will be quite accurately known from the precisely measured value for e_{aq}^-.[71]

The other factor in the Smoluchowski equation is the reaction distance. Usually, the reaction distance is taken to be the summation of the radii of the two reactants. However, the e_{aq}^- reactions studied here are electron-transfer reactions. It is possible that the e_{aq}^- reactions occur at rather long distances. Indeed, there are a few examples of e_{aq}^- reactions that have long reaction distances.[71,73] Therefore, it is difficult to assume certain reaction distances a priori in the Smoluchowski analysis of the e_{aq}^- reactions.

Instead, tentative reaction distances will be determined from the Smoluchowski equation with the rate constants measured in the experiments, a spin factor of $^1/_4$, and the mutual diffusion constants. The reaction distances so determined will be reviewed to see whether or not the e_{aq}^- reactions with the radicals are indeed diffusion controlled with a spin factor of $^1/_4$.

The Smoluchowski analysis can be implemented immediately for the e_{aq}^- reactions with neutral radicals. When the counter radical is charged, the observed rate constant has to be corrected for the ionic strength first. The ionic strength correction is made with the extended Debye−Hückel theory.[74]

$$\log k_0 = \log k_{obs} - Z_1 Z_2 A\sqrt{I}/(1 + BR\sqrt{I}) \quad (4)$$

$$A = (F^3/4\pi N_A \ln 10)(\rho/2)^{1/2}(\epsilon\epsilon_0 k_B N_A T)^{-3/2} \quad (5)$$

$$B = (2F^2\rho/\epsilon\epsilon_0 k_B N_A T)^{1/2} \quad (6)$$

Here, k_0 is the corrected rate constant, k_{obs} is the observed rate constant, Z_1 and Z_2 are the numbers of charge of the two reactants, I is the ionic strength, R is the reaction distance, F is the Faraday constant, N_A is Avogadro's number, ρ and ϵ are the density and dielectric constant of the medium, ϵ_0 is the vacuum permittivity, k_B is the Boltzmann constant, and T is the temperature. The ionic strength correction requires the reaction distance, so an iterative procedure must be invoked to obtain it.

Table 7 shows the reaction distances at room temperature derived from the Smoluchowski equation. All the reaction distances are either comparable to or longer than the summation of the radii of the two reactants (see Table 6). Some of the reactions have rather long reaction distances of up to ~10 Å. These reactions may be long-range electron transfer (see also discussion below). Such a reaction distance is not unusual for e_{aq}^- reactions. For instance, it has been reported that the reaction distances of the e_{aq}^- reactions with nitrobenzene, molecular bromine, and molecular iodine are 8.5, 10, and 11 Å, respectively.[71,73] However, some reaction distances in Table 7 are even larger. There does not seem to be any precedent for such long reaction distances for rapid bimolecular reaction in solution. These systems involve $^{\bullet}OH$, $^{\bullet}N_3$, $Br_2^{\bullet -}$, $I_2^{\bullet -}$, and $C_6H_5S^{\bullet}$. Some assumption made in the analysis of these systems must be wrong. In light of the accuracy of the estimate of the mutual diffusion constant, only the values of the spin factor can be in

TABLE 7: Summary of Hydrated Electron Reactions with Various Radicals

radicals	k_{obs} (M^{-1} s^{-1}) at 298 K[a]	E_{app} (kJ mol^{-1})[b]	R (Å) at 298 K with $\sigma = 1/4$[c]	ΔG (eV)[d]	reorganization energy (eV)[e]
•OH	3.2×10^{10}	16.3 ± 1.0	24.2	−4.76	3.3
•$C(CH_3)_2OH$	5.3×10^{9}	20.2 ± 1.1	4.7		2.6
(•CH_2)$(CH_3)_2COH$	5.6×10^{9}	23.1 ± 1.0	5.1	−2.30	2.6
•CO_2^-	5.6×10^{9}	20.9 ± 0.3	7.7	−1.59	4.4
•SO_3^-	6.3×10^{9}	19.5 ± 1.1	8.5	−3.60	3.8
CO_3•$^-$	4.9×10^{9}	17.9 ± 1.1	7.1	−4.46	3.1
•C_6H_6OH	1.1×10^{10}	17.6 ± 1.2	9.7	−2.85	3.1
Br_2•$^-$	1.9×10^{10}	16.0 ± 2.5	19.0	−4.50	2.7
I_2•$^-$	2.8×10^{10}	10.4 ± 1.0	26.1	−3.90	2.6
•N_3	2.4×10^{10}	15.2 ± 1.1	18.9	−4.20	2.9
C_6H_5O•	1.1×10^{10}	20.8 ± 2.5	9.7	−3.66	2.2
p-$(H_3C)C_6H_4O$•	1.3×10^{10}	19.9 ± 1.8	10.9	−3.56	2.2
p-OC_6H_4O•$^-$	6.2×10^{9}	22.1 ± 2.5	9.1	−2.90	2.3
C_6H_5S•	3.1×10^{10}	22.5 ± 3.8	27.3	−3.56	2.2

[a] Rate constants at 298 K were obtained from the linear fitting of log k vs T^{-1}. Where appropriate, the rate constants were corrected for ionic strength as explained in the text. A tentative reaction distance of 10 Å was assumed for the ionic strength correction in the systems of Br_2•$^-$ and I_2•$^-$ radicals. Typically, the second-order rate constants have statistical errors of ±10%. For the phonolate systems, the error bars are ±20%. [b] Apparent activation energy. The error is from the least-squares fitting procedure. [c] Reaction radius under the assumption of a spin factor of 1/4. [d] Free energy difference for the reactions determined from the reduction potentials of the reactants. For the reduction potentials, see refs 13−15 (e_{aq}^-), 199 (•OH and Br_2•$^-$), 200 ((•CH_2)$(CH_3)_2COH$, •CO_2^- and •C_6H_6OH), 201 and 202 (•SO_3^-), 203 (CO_3•$^-$), 204 (I_2•$^-$), 205 (•N_3), 16 (C_6H_5O• and *p*-$(H_3C)C_6H_4O$•), 206 (*p*-OC_6H_4O•$^-$), and 141 (C_6H_5S•) [e] Solvent reorganization energies were estimated from eq 8 with reactant radii from Table 6 and reaction radii shown above. For systems where $\sigma \gg 1/4$, a tentative reaction radius of 10 Å was used for the estimation. See Supporting Information for further comments and additional contributions of internal reorganization energies.

question. The spin factor would have to be significantly larger than 1/4 in those systems in order to bring the values of the reaction distance down to plausible ones near 10 Å.

If triplet radical pairs instead of singlet pairs were engaged in reaction, then the spin factor would be 3/4. This interpretation is hard to accept because no triplet state of the reaction products is easily accessible in these systems (but see the discussion for the e_{aq}^- reaction with C_6H_5S• in the next section). Alternatively, the spin factor could approach unity if rapid singlet−triplet conversion took place during radical−radical encounters. Two situations are possible. If one (or both) of the two reactant radicals had a fast spin relaxation rate, then the singlet−triplet conversion for the radical pairs would also be fast. Alternatively, the radical pair could undergo singlet−triplet interconversion by the heavy atom effect. The interconversion must take place within the radical pair lifetime in order to produce large spin factors.

An estimate of the relevant time scale can be made with the theory of Brownian motion. It takes a time of $r^2/6D$ for the two molecules whose mutual diffusion constant is D to diffuse apart by a mean distance of r.[75] For the present purposes, the initial radical pair can be one with a triplet (or nonreactive) spin state in contact. With a mutual diffusion constant like that of the e_{aq}^-/•OH radical pair, it would take 24 ps at room temperature to reach a mean-square separation of 10 Å. If the singlet−triplet interconversion occurred in that time, then reaction would be possible because the reaction distances can be of that magnitude.

Most of the radicals studied in this work have spin relaxation times near 1 μs (Table 6) and should react with a spin factor of 1/4. The spin relaxation times of •CO_2^- and CO_3•$^-$ can be estimated to be on the order of 10 ns from their broader ESR linewidths.[76] These spin relaxation processes are still slow compared to the radical pair lifetime, so the spin factors for reactions with these two radicals are also most likely to be 1/4.

The spin relaxation times of five of the radicals are unknown because no ESR spectrum has been observed for these radicals in aqueous solutions at room temperature. These radicals are •OH, •N_3, Br_2•$^-$, I_2•$^-$, and C_6H_5S•. It is likely that the spin relaxation rates of these radicals are so fast that the ESR spectra become too broad to be detected. It is interesting to notice that spin factors of much larger than 1/4 (that is, the apparent reaction distances in Table 7 are ≫10 Å) have been found in the e_{aq}^- reactions with all of these radicals. The spin relaxation mechanisms of these radicals will be discussed below.

Both •OH and •N_3 are linear, and their unpaired electron resides in a degenerate π orbital in vacuum.[77] The spin−orbit coupling provides a connection of the spin to the molecular axis so that molecular tumbling will cause spin relaxation. In aqueous solutions, the degenerate orbitals can be dynamically perturbed and the degeneracy removed by the interaction with water molecules surrounding the radicals. The orbital angular momentum is thus quenched. All of these effects can contribute to the spin relaxation. Unfortunately, no analytical treatment of this spin relaxation mechanism has been reported to estimate the relaxation time. Nevertheless, fast spin relaxation of these radicals has been inferred in the literature.

In the case of •OH, a spin relaxation time in solution of <1 ns has been estimated from spin population transfer during •OH reaction in time-resolved ESR measurements.[78] The ESR spectrum of •OH has been observed in ice at low temperature.[79−81] The solid matrix restricts the motion of the solvent molecules, while the degeneracy of the π orbitals is removed by a preferential hydrogen bonding. It has been found that the anisotropic g-factor of •OH is sensitive to the solvating environment.[82] Recently, spectroscopic investigations of •OH−H_2O complex in the gas phase and in argon matrices have been reported, and they provide important information about its molecular as well as electronic structure.[83−87]

Fast spin relaxation of •N_3 has been discussed in reference to photochemical systems.[88] Photolysis of dye molecules produced their excited triplet states, which were subsequently quenched by bimolecular reactions with azide anion. The quenching process possibly involved charge transfer, but the yields of •N_3 and the radical anion of the dye molecule were found to be small. The quenching could indeed form geminate pairs of the radical anion of the dye and •N_3. These geminate pairs would initially be triplet, reflecting the spin multiplicity of the precursor, the triplet state of the dye molecule. However, efficient spin relaxation of •N_3 could convert the triplet geminate pairs into singlet rapidly before the two radicals would separate

by diffusion. Then, the subsequent back reaction of the singlet geminate pairs to form the ground singlet state of the dye molecule and azide anion could ensue, and the escape yield of $^{\bullet}N_3$ would be diminished. This quenching by azide anion was compared with that by nitrite anion. Nitrite anion also quenched the triplet states as efficiently as azide anion did, but a large yield of nitrite radical ($^{\bullet}NO_2$) resulted from the quenching reaction. The $^{\bullet}NO_2$ is a bent species, and there is no definite orbital angular momentum available for the radical. Thus, the $^{\bullet}NO_2$ and the dye radical anion in the triplet geminate pairs formed in the quenching reaction would most probably diffuse apart without fast conversion into singlet pairs.[89] A similar type of spin−orbit effect has been reported in the quenching of the excited states of organic molecules by halide anions as well.[90,91] It is interesting to note that no ESR spectrum has been detected for $^{\bullet}N_3$ even in low-temperature solid matrices.[92] Azidyl radical is a neutral species, and its unpaired electron resides in a nonbonding degenerate π orbital. Strong perturbation by solvating molecules may be absent in such a system because of the lack of energy gain through the perturbation.

The analysis of the rate constants of the self-reactions with the Smoluchowski equation also supports fast spin relaxation of $^{\bullet}OH$ and $^{\bullet}N_3$. In contrast with the e_{aq}^- reactions with radicals, the two reactants must be in contact for the self-reactions of $^{\bullet}OH$ and $^{\bullet}N_3$ to take place. Thus, the reaction distances for the self-reactions can be reasonably estimated. With the rate constant determined in the experiments (see Supporting Information), the mutual diffusion constant, and the reaction distance, the Smoluchowski analysis can provide estimates of the spin factors for the self-reactions. Such an analysis yields spin factors of 0.81 and 0.64 for the self-reactions of $^{\bullet}OH$ and $^{\bullet}N_3$, respectively, in aqueous solution at room temperature. These large spin factors are in accord with the idea that efficient spin relaxation operates for the two radicals. We note that Elliot et al. have discussed the $^{\bullet}OH + {}^{\bullet}OH$ reaction under the assumption that the spin factor is unity and argued that the rate is about a factor of 2 less than that predicted for diffusion control.[52,93]

The spin relaxation mechanism for $C_6H_5S^{\bullet}$ may be analogous to those for $^{\bullet}OH$ and $^{\bullet}N_3$. It is useful to compare the electronic structure of $C_6H_5S^{\bullet}$ with that of $C_6H_5O^{\bullet}$. Resonance Raman spectra have been measured for these two radicals in aqueous solution, and the structure of the two radicals has been discussed.[94−96] The C−O bond in $C_6H_5O^{\bullet}$ has a bond order of 1.5, indicative of the delocalization of the unpaired electron over the π system of the aromatic ring. On the other hand, the C−S bond in $C_6H_5S^{\bullet}$ has a single-bond character, and the unpaired electron in $C_6H_5S^{\bullet}$ is likely to be localized on the sulfur atom. The narrow line width of the ESR spectrum of $C_6H_5O^{\bullet}$ in aqueous solution at room temperature suggests that the spin relaxation time is around 1 μs.[97−99] ESR spectra of $C_6H_5S^{\bullet}$ have never been unequivocally observed in aqueous solution at room temperature.[4,100] ESR spectra have been reported for $C_6H_5S^{\bullet}$ deposited on a cold finger.[101−105] The highly anisotropic *g*-factor found in the spectra also indicates a high degree of the localization of the unpaired electron on the sulfur. If the unpaired electron of $C_6H_5S^{\bullet}$ were totally localized on the sulfur atom, then the unpaired electron would be in a sulfur-degenerate 3p orbital in the absence of solvent perturbation. In this view, the unpaired electron in $C_6H_5S^{\bullet}$ would also be subject to spin−orbit coupling, analogous to $^{\bullet}OH$ and $^{\bullet}N_3$.

The analysis of the rate constants of the self-reactions of $C_6H_5S^{\bullet}$ and $C_6H_5O^{\bullet}$ in aqueous solutions (see Supporting Information) with the Smoluchowski equation yields spin factors of 0.53 and 0.29, respectively, at room temperature. The spin factor for the $C_6H_5O^{\bullet}$ self-reaction is very close to $^1/_4$ as expected. The difference in the spin factors may arise from a difference in the spin relaxation rate of the two radicals.

Fast spin relaxation of $C_6H_5S^{\bullet}$ was also proposed in magnetic field effect studies.[106] Photosensitization of diphenyl disulfide produced the excited triplet state, from which the sulfur−sulfur bond cleavage took place to generate a geminate $C_6H_5S^{\bullet}$ pair inside a micellar cage. The rate constant of the recombination reaction of $C_6H_5S^{\bullet}$ was found to be independent of external magnetic field up to 1 T. In the case of carbon-centered organic radicals, recombination of triplet geminate radical pairs usually decelerates upon the application of external magnetic field because the removal of the degeneracy of the triplet sublevels due to the Zeeman effect suppresses the hyperfine mixing between the triplet and singlet radical pairs.[107,108] The absence of a magnetic field effect for the $C_6H_5S^{\bullet}$ pairs was ascribed to fast spin relaxation of the radical.

Dihalogen radical anions are σ radicals.[77] Thus, their spin relaxation mechanisms have contributions from spin-rotation, hyperfine anisotropy, and quadrupole anisotropy.[109] Analysis of these mechanisms suggests that spin-rotation is the most effective[110,111] but that relaxation times in the range of 1−10 ns are likely for $Br_2^{\bullet-}$ and $I_2^{\bullet-}$ and are not short enough to affect the spin factor very much.

In addition to spin relaxation of individual radicals, there is also the possibility of singlet−triplet conversion in the radical pair from the heavy-atom effect. Steiner and Winter studied the reductive quenching of the excited triplet state of thionine by halogen-substituted anilines.[112] They found that the yield of the aniline radical cation decreased as the atomic number of the halogen increased while the quenching rate constant was almost constant irrespective of the type of halogen substituent. They explained this observation with the spin−orbit coupling effect of the halogen group. A triplet exciplex composed of thionine radical and aniline radical cation is formed immediately after the quenching reaction. This triplet exciplex can possess electronic overlap with the ground singlet states of thionine and aniline through the spin−orbit coupling operator. As the atomic number of the halogen increases, so does the spin−orbit coupling coefficient. Therefore, the electronic coupling becomes larger with the atomic number of the halogen. When the electronic coupling is large enough, the triplet exciplex decays to form the ground singlet states of thionine and aniline before the two radicals separate from each other by diffusion.

The heavy-atom spin−orbit coupling effects have been observed not only in a number of photochemical geminate processes[113−122] but also for bimolecular reactions between halogen-substituted aniline radical cation and an organic radical.[115] Thus, it is possible that, during diffusive encounters of e_{aq}^- and $Br_2^{\bullet-}$ or $I_2^{\bullet-}$, triplet pairs could be electronically mixed with the singlet ground state of the product (Br^- or I^-) and they react before the two radicals separate from each other by diffusion.

The spin factors for the self-disproportionation reactions of $Br_2^{\bullet-}$ and $I_2^{\bullet-}$ can be estimated to be 0.83 and 1.03, respectively, at room temperature from the Smoluchowski analysis of the rate constants (see Supporting Information). Thus, it is probable that the effect of heavy-atom spin−orbit coupling operates also for the self-disproportionation reactions. Indeed, the unusual magnetic field effect observed for the self-disproportionation reaction of $Br_2^{\bullet-}$ has been attributed to this effect.[123]

It is helpful to use a theoretical model developed by Mints and Pukhov[124] to analyze the relationship between the spin relaxation rate and the enhanced spin factors. They derived an

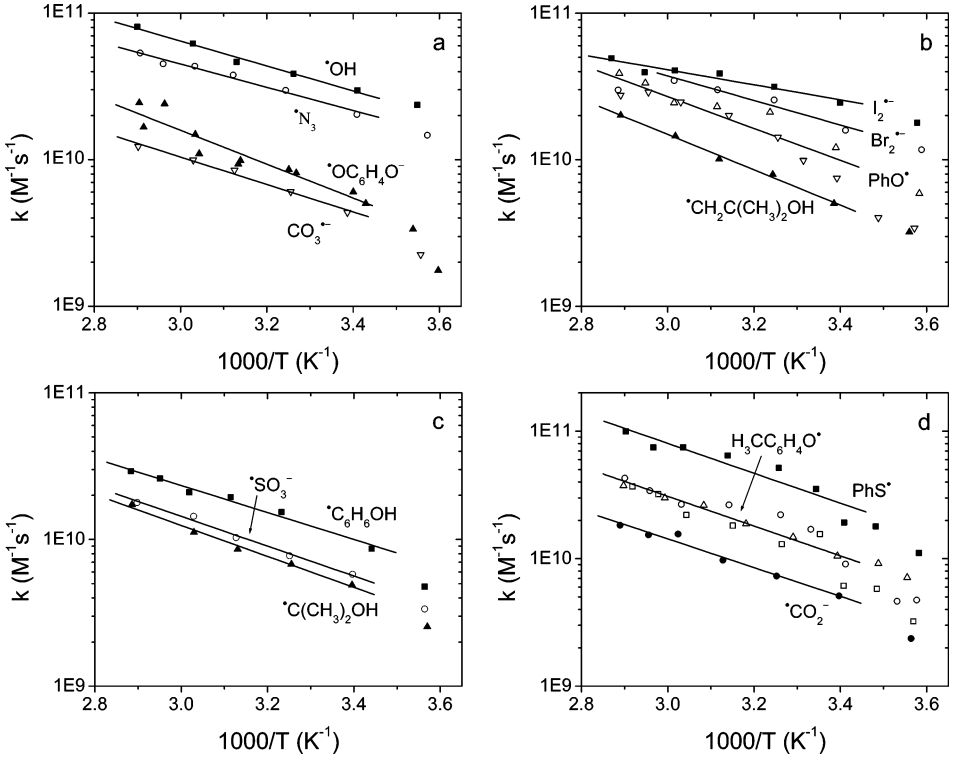

Figure 4. Arrhenius plots of the rate constants (corrected for ionic strength) of the e_{aq}^- reactions with various radicals as marked: (a) •OH, $•N_3$, $•OC_6H_4O^-$, $CO_3•^-$; (b) $I_2•^-$, $Br_2•^-$, PhO• ($Br_2•^-$oxidation, ▽), PhO• ($•N_3$ oxidation, △), $•CH_2C(OH)(CH_3)_2$; (c) $•C_6H_6OH$, $•SO_3^-$, $•C(OH)(CH_3)_2$; (d) PhS•, $H_3CC_6H_4O•$, $•CO_2^-$. For $H_3CC_6H_4O•$, three sets of data are included: oxidation by $Br_2•^-$ (□), oxidation by $•N_3$ (○), and photo-oxidation (△).

analytical expression for the spin factor (σ) from the stochastic Liouville equation, which incorporated phenomenological spin relaxation of the reactant radicals.

$$\sigma = \frac{1}{2}\cdot\frac{k\tau PQ}{k\tau(P+Q)+2PQ} \tag{7}$$

where

$$\tau = ab/D$$

$$P = 2\cdot\frac{1+\sqrt{2x}}{2+\sqrt{2x}}$$

$$Q = 1+\sqrt{y}$$

$$x = \frac{1}{2T_1}\cdot\frac{b^2}{D}$$

$$y = \frac{1}{T_2}\cdot\frac{b^2}{D}$$

Here, k is the rate constant of the radical pair reaction, τ is the radical pair lifetime, a is the thickness of the reaction layer, b is the reaction distance, D is the mutual diffusion constant, and T_1 and T_2 are the longitudinal and transverse spin relaxation times of the counter radical. This expression assumes that the spin relaxation of e_{aq}^- is much slower than that of the counter radical. Also, hyperfine interaction and Zeeman interaction are ignored (see ref 17).

Assuming reaction distances of 8 Å for the e_{aq}^- reactions with •OH and $•N_3$ and 10 Å for those with $C_6H_5S•$, $Br_2•^-$, and $I_2•^-$, the spin factors can be evaluated to be 0.76, 0.59, 0.68, 0.48, and 0.65 for these reactions, respectively, at 298 K, according to the Smoluchowski analysis (Table 7). If these spin factors are substituted in eq 7, with a reasonable assumption of $a = 2$ Å and $k = 3 \times 10^{12}$ s^{-1}, then the spin relaxation times[125] (or singlet−triplet conversion times) can be estimated to be 0.8, 9, 5, 40, and 6 ps for these radicals, respectively.

Temperature Dependence of the Diffusion-Controlled e_{aq}^- Reactions. Table 7 lists the apparent activation energies[63] for the e_{aq}^- reactions with radicals obtained from an Arrhenius fitting of the rate constants, as shown in Figure 4. The rate constants for temperatures below about 17 °C were discarded in derivation of the apparent activation energies because it has been found that the Arrhenius plot of e_{aq}^- diffusion is quite linear over the temperature range of 15−75 °C but has a curved profile below 15 °C.[70,71] The data for the Arrhenius plots are given in Table 3 for •OH and in Table S3 of Supporting Information for the other radicals. In the cases of charged counter radicals, the plots were made with the rate constants after corrections for the ionic strengths.

Many of the apparent activation energies in Table 7 are about 20 kJ mol^{-1} within ±3 kJ mol^{-1}. Such a value is expected if the e_{aq}^- reactions are diffusion-controlled for the following reason. As mentioned previously, the diffusion of e_{aq}^- is much faster than that of the counter-radicals at room temperature. Therefore, the mutual diffusion constant in the Smoluchowski equation is dominated by the diffusion constant of e_{aq}^- at room temperature. The activation energy of e_{aq}^- diffusion is 20.25 ± 0.08 kJ mol^{-1} over the temperature range from 15 to 75 °C.[70,71] Although the activation energies for diffusion of the other radicals are not known, values for various related stable species are not larger than 20.25 kJ mol^{-1}.[93] Thus, the e_{aq}^- diffusion should dominate the mutual diffusion constant over the whole temperature range in our study. If, among the factors on the right-hand side of the Smoluchowski equation (eq 1), only the mutual diffusion constant is a function of temperature, then the apparent activation energy of a diffusion-controlled reaction should be equal to the activation energy of the mutual diffusion, which must be close to that of e_{aq}^- diffusion.

The analysis of the rate constants at room temperature in the last section has led to the conclusion that the e_{aq}^- reactions with some radicals are diffusion controlled with a spin factor of $^1/_4$. These systems are $^{\bullet}SO_3^-$, $CO_3^{\bullet-}$, $^{\bullet}CO_2^-$, $^{\bullet}C(CH_3)_2OH$, $(^{\bullet}CH_2)(CH_3)_2COH$, $^{\bullet}C_6H_6OH$, $C_6H_5O^{\bullet}$, *p*-$(H_3C)C_6H_4O^{\bullet}$, and *p*-$OC_6H_4O^{\bullet-}$. All of these reactions have apparent activation energies within ± 3 kJ mol^{-1} of 20 kJ mol^{-1}. Thus, both the magnitude of the rate constant at room temperature and the temperature dependence of the rate constant suggest that these reactions are diffusion controlled with a spin factor of $^1/_4$.

Some apparent activation energies in Table 7 are significantly smaller than 20 kJ mol^{-1}. These cases are for $^{\bullet}OH$, $^{\bullet}N_3$, $Br_2^{\bullet-}$, and $I_2^{\bullet-}$. The relatively small apparent activation energies seem to imply that these e_{aq}^- reactions are not diffusion controlled. However, the large values of the rate constant (or apparent reaction distance in Table 7) suggest otherwise. If the intrinsic rate constants do not interfere with the observed rate constants, either (or both) the reaction distance or the spin factor must be temperature dependent.

Schmidt et al. discussed the temperature dependence of the rate constants of the e_{aq}^- reaction with nitrobenzene ($C_6H_5NO_2$), where the spin factor is not an issue (i.e., $\sigma = 1$).[71,126] The rate constant of this reaction is 3.8×10^{10} M^{-1} s^{-1} at room temperature, and the activation energy is 17 kJ mol^{-1} up to 100 °C.[127] The Smoluchowski analysis indicates that the $e_{aq}^- + C_6H_5NO_2$ reaction is diffusion controlled, but this electron transfer has a rather long reaction distance of 8.5 Å at room temperature.[71] An important factor in this electron-transfer reaction is a rather large free energy change (ΔG) of -2.38 eV.[71] Thus, the long-range reaction is most probably assisted by the solvent reorganization energy.[128]

$$\lambda_{out} = \frac{e^2 N_A}{4\pi\epsilon_0}\left(\frac{1}{2r_A} + \frac{1}{2r_B} - \frac{1}{R}\right)\left(\frac{1}{\epsilon_{op}} - \frac{1}{\epsilon_s}\right) \qquad (8)$$

Here, e is the electric charge, N_A is Avogadro's number, ϵ_0 is the vacuum permittivity, r_A and r_B are the radii of the two reactants, R is the reaction distance, and ϵ_{op} and ϵ_s are the optical and static dielectric constants.

When a reaction probability is an exponential function of reaction distance, an analytic solution of the diffusion equation is available.[129,130] Then, the effective reaction distance is a function of the mutual diffusion constant, and a larger diffusion constant makes the effective reaction distance shorter. The analysis by Schmidt et al. concludes that the reaction distance for the $e_{aq}^- + C_6H_5NO_2$ reaction decreases from 8.5 Å at room temperature to 7.3 Å at 80 °C.[71] This change partially compensates for the increase in diffusion rate, reducing the apparent activation energy to 17 kJ mol^{-1}.[131] In general, the influence of diffusion on the effective reaction distance for bimolecular reactions has been demonstrated in the analysis of fluorescence quenching systems.[132]

Some e_{aq}^- + radical reactions have rather long reaction distances at room temperature, and there is a chance that they may have temperature-dependent reaction distances. For instance, the $e_{aq}^- + {}^{\bullet}C_6H_6OH$ reaction has a long reaction distance of 9.7 Å at room temperature, and the apparent activation energy is 17.6 kJ mol^{-1}, slightly smaller than that of e_{aq}^- diffusion. For the e_{aq}^- reactions with *p*-$(H_3C)C_6H_4O^{\bullet}$ and *p*-$OC_6H_4O^{\bullet-}$, the reaction distances are 10.9 and 9.1 Å, respectively, but both apparent activation energies are 20 kJ mol^{-1} within experimental error. It should be mentioned that all of these reactions have large magnitudes of ΔG (Table 7).

It is possible that the temperature dependence of the average reaction distance contributes to some extent to the temperature dependence of the observed rate constants of the e_{aq}^- reactions with $^{\bullet}OH$, $^{\bullet}N_3$, $Br_2^{\bullet-}$, and $I_2^{\bullet-}$. It is very difficult to give quantitative estimates on such an effect because it requires a precise analytical form of the reaction probability as a function of reaction distance.[129,133] On the basis of the behavior of the $e_{aq}^- + C_6H_5NO_2$ reaction,[71] however, the activation energies of 10−16 kJ mol^{-1} for $^{\bullet}OH$, $^{\bullet}N_3$, $Br_2^{\bullet-}$, and $I_2^{\bullet-}$ seem too low to be explained by this effect alone.

We propose that the spin factors for these reactions also change with temperature. Such an effect could arise from a competition between diffusive separation and spin dynamics during e_{aq}^- + radical encounters. The radical pair lifetime can be assumed to be inversely proportional to the mutual diffusion constant (D).[48] The temperature dependence of D is such that it changes by about a factor of 3 between 25 and 70 °C so the radical pair lifetime should decrease by about that factor.

As explained in the last section, for the systems involving $^{\bullet}OH$ and $^{\bullet}N_3$, rapid singlet−triplet conversion is most probably induced by fast spin relaxation of the radicals during their encounter with e_{aq}^-. Because the relaxation mechanisms of these radicals have never been analytically clarified, it seems impossible to estimate the temperature dependence of their spin relaxation. However, if the spin relaxation were only weakly temperature dependent (or, in the line narrowing region, actually slower at higher temperature), then the spin factor could change with temperature. At higher temperatures, diffusive separation of triplet radical pairs would be more rapid and could be faster than the spin relaxation processes. A lower spin factor at higher temperature would lead to a lower effective activation energy. This explanation is in agreement with our experimental findings qualitatively.

The same argument can apply to the dihalogen radical anion systems. As discussed earlier, effective singlet−triplet conversion for $e_{aq}^-/Br_2^{\bullet-}$ or $I_2^{\bullet-}$ radical pairs operates only during the radical pair lifetime because substantial electronic overlap between the radicals is required. Therefore, as the radical pair lifetime gets shorter at higher temperature, there is less singlet−triplet conversion, which means a lower spin factor for the reactions.

The temperature dependence of the spin factor can be discussed based on the formulation by Mints and Pukhov.[124] Figure 5 shows Arrhenius plots of the second-order reaction rate constants, with spin factors evaluated according to eq 7. It should be pointed out that only the mutual diffusion constant is temperature dependent in this model with an activation energy of 20.25 kJ mol^{-1}. Nearly linear Arrhenius plots were obtained over our temperature range, and the apparent activation energy for the second-order reaction was indeed lowered to about 16 kJ mol^{-1} due to the temperature dependence of the spin factor. The very low value of 10.4 kJ mol^{-1} for $I_2^{\bullet-}$ probably cannot be explained by this process alone and suggests that both the spin factor and the reaction distance are changing with temperature. If this is so, then changes in spin factor may also be involved for the other radicals with activation energies significantly lower than 20 kJ mol^{-1}.

This analysis of the spin dynamics for the e_{aq}^- + radical reactions parallels that for geminate back electron-transfer in photogenerated triplet radical pairs of $Ru(bpy)_3^{3+}$ and methylviologen radical cation ($MV^{\bullet+}$).[134,135] The viscosity dependence of the radical yield of the photochemical reaction has been explained by competition between spin relaxation, which converts the geminate triplet pairs into singlet pairs from which back electron-transfer ensues rapidly and diffusive separation of the radicals occurs. The same idea applies to the comple-

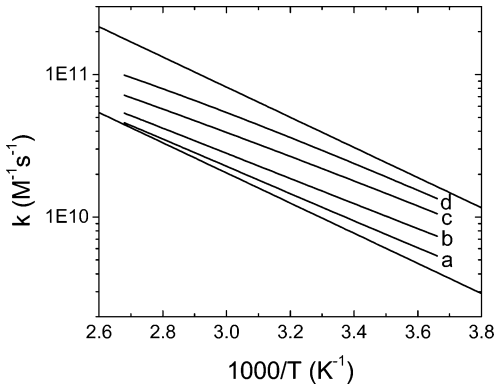

Figure 5. Arrhenius plots of second-order rate constants for e_{aq}^- + radical reactions calculated according to eqs 1 and 7. Only the diffusion constant has been assumed to be temperature dependent in these calculations. Parametrizations of eqs 1 and 7 are $k = 3 \times 10^{12}$ s^{-1}, $a = 2$ Å, $b = 8$ Å, $D = 6.0 \times 10^{-9}$ m^2 s^{-1} at 298 K with an activation energy of 20.25 kJ mol^{-1}, and the spin relaxation times, assuming $T_1 = T_2$, of 1 ns (a), 100 ps (b), 10 ps (c), and 1 ps (d). The upper and lower lines represent temperature-independent spin factors of 1 and $^1/_4$, respectively. The apparent activation energies over the temperature interval 0−100 °C ($1/T = 0.00268-0.00366$) are 18.3, 16.9, 16.2, and 16.9 kJ mol^{-1}, for curves (a) through (d), respectively. The vertical position of a curve at a particular temperature relative to the lines for spin factors of $^1/_4$ and 1 represents the spin factor at that temperature.

mentary magnetic field dependence of the radical yield, where the rate of the spin process is varied while the diffusion rate is constant. A theoretical analysis[135] indicates that such an effect of spin dynamics can be observed only when the geminate reaction is controlled by diffusion.[136] Diffusion control is assumed also in our analysis of homogeneous e_{aq}^- + radical reactions. An analogous viscosity dependence has been found for geminate systems where heavy-atom spin−orbit coupling effects are important.[117] It should be mentioned that detailed theoretical analysis of the spin dynamics in radical pair geminate recombination has been reported recently.[137−139]

In the previous section, the spin relaxation of $C_6H_5S^•$ was discussed with respect to spin−orbit interaction, analogous to $^•OH$ and $^•N_3$. The apparent activation energy for the e_{aq}^- + $C_6H_5S^•$ reaction was found to be around 22 kJ mol^{-1} (Table 7). This value is quite different from those for the e_{aq}^- reactions with $^•OH$ and $^•N_3$ and suggests that the spin factor remains approximately constant (0.68 at room temperature and a reaction distance of 10 Å) regardless of temperature.

These observations may indicate that the excited triplet state is formed in the e_{aq}^- + $C_6H_5S^•$ reaction. The energy of the excited triplet state of the benzenethiolate anion ($C_6H_5S^-$) was determined to be 3.1 eV from the phosphorescence measurement for $C_6H_5S^-$ in a frozen aqueous matrix at 77 K.[140] The ΔG for the e_{aq}^- reaction with $C_6H_5S^•$ to form the $C_6H_5S^-$ ground state is 3.56 eV, estimated from the reduction potentials of e_{aq}^- (−2.87 V)[13−15] and $C_6H_5S^•$ (+0.69 V).[141] Thus, it is possible energetically that the reaction proceeds to yield the excited triplet state, although there is not a large driving force for this reaction.

Now that temperature dependence of these e_{aq}^- + radical reactions has been analyzed, we briefly discuss a few other relevant systems reported in the literature. As mentioned in the Introduction, the rate constants of the e_{aq}^- + $^•H$ reaction has been reported.[21,22] The rate constant is 2.4×10^{10} M^{-1} s^{-1} at room temperature and its apparent activation energy is 14 kJ mol^{-1} over a temperature range from 20 to 250 °C.[22] Contrary to our e_{aq}^- + radical systems, the diffusion constant of $^•H$, 7.7×10^{-9} m^2 s^{-1},[72,142,143] is larger than that of e_{aq}^- at room temperature, but it has a smaller activation energy of 12 kJ mol^{-1}.[143] The spin relaxation time for $^•H$ is at least 10 μs.[144] The Smoluchowski analysis suggests that the e_{aq}^- + $^•H$ reaction is indeed diffusion controlled with a spin factor of $^1/_4$.

The self-reaction of e_{aq}^- is another example. The rate constant ($2k$) of the e_{aq}^- + e_{aq}^- reaction is 1.0×10^{10} M^{-1} s^{-1} at room temperature.[23,60] The temperature dependence of the rate constant has an apparent activation energy of 20.3 kJ mol^{-1} up to 150 °C, but then the reaction slows down at higher temperatures.[23,60] The Smoluchowski analysis suggests that the reaction is diffusion controlled with a spin factor of $^1/_4$ up to 150 °C. The kinetic behavior above 150 °C seems to originate from the reaction mechanism, i.e., formation of a transient species in the course of the reaction.[71,145]

The spin factor for the e_{aq}^- + O_2 reaction has been discussed in the literature.[71] The ground state of O_2 is a triplet. Therefore, at random encounters between e_{aq}^- and O_2, there are probabilities of $^1/_3$ to form doublet pairs and $^2/_3$ to form quartet pairs. Because the product of the reaction, the ground state of the superoxide radical anion, is doublet, the proper spin factor for this reaction appears to be $^1/_3$. Schmidt et al. discussed that two of the four substates of the quartet pair could convert into the doublet pair states during the encounter through the zero-field splitting Hamiltonian for O_2.[71] Their conclusion was that the correct spin factor for the reaction should be $^2/_3$, and the temperature dependence of the reaction distance was considered to explain the observed rate constants, 1.9×10^{10} M^{-1} s^{-1} at room temperature, and its apparent activation energy of 13.1 kJ mol^{-1} over a temperature range of 20−200 °C. However, if the spin conversion rate had the right magnitude, then there could be a competition between spin conversion and pair separation.[146] In light of our findings in the present study, it is quite possible that the spin factor also affects the temperature dependence of this rate constant.

Buxton and Elliot[52,93] examined the $^•OH$ + $^•OH$ and $^•H$ + $^•OH$ reactions in aqueous solution over a temperature range of 20−200 °C and analyzed the observed rate constants, k_{obs}, with the following equation.[47]

$$k_{obs}^{-1} = k_{act}^{-1} + k_{diff}^{-1} \quad (9)$$

Here, k_{act} is the intrinsic reaction rate constant, and k_{diff} is the diffusion-controlled rate constant. In their estimate of the diffusion-controlled rate constants, a spin factor of 1 was used, assuming fast spin relaxation of $^•OH$. Although this is a possibility, the spin factor may change for these reactions over the temperature range. If the observed rate constants are taken in the Smoluchowski equation, then the resultant spin factor will be 0.81 and 0.54 at room temperature for the $^•OH$ + $^•OH$ and $^•H$ + $^•OH$ reactions, respectively. Their analysis assumes that the activation energy of the diffusion-controlled rate constant is that of water self-diffusion, 17.6 kJ mol^{-1}. It should be remembered that the diffusion constant of $^•H$ (7.7×10^{-9} m^2 s^{-1})[72,142,143] is much larger than that of $^•OH$ (2.0×10^{-9} m^2 s^{-1})[72] at room temperature and the activation energy of $^•H$ diffusion has been reported to be 12 kJ mol^{-1}.[143] Thus, their analysis of the $^•H$ + $^•OH$ reaction should be viewed with caution. On the other hand, it is interesting to note that good agreement between the gas phase and aqueous solution has been observed with respect to kinetics of the $^•OH$ + $^•OH$ reaction in their analysis.[93]

So far, our analysis of the e_{aq}^- + radical reactions has assumed that the intrinsic rate constant (k_{act} in eq 9) is much larger than the diffusion-controlled rate constant (k_{diff}). One can argue that the relatively low apparent activation energies found for the e_{aq}^- reactions with $^•OH$, $^•N_3$, $Br_2^{•-}$, and $I_2^{•-}$ may reflect

a contribution of k_{act} to k_{obs} in eq 9. We briefly discuss this possibility below.

It is clear in Table 7 that the e_{aq}^- reactions with $^{\bullet}OH$, $^{\bullet}N_3$, $Br_2^{\bullet-}$, and $I_2^{\bullet-}$ are all highly exoergic. Even though a large solvent reorganization energy (eq 8) is possible (~2 eV) when these electron-transfer reactions take place at a long distance (~10 Å), they most likely lie in the Marcus inverted region. In the inverted region, the electron-transfer rate decreases as the magnitude of the free energy difference (ΔG) increases.[147−149] Also, because nuclear tunneling may be activationless in the inverted region, the electron-transfer rate in the inverted region is not as temperature dependent as in the normal region.[149−151] These considerations cast doubt on the assumption, $k_{act} \gg k_{diff}$.

Generally, it is very difficult to characterize electron transfer in the inverted region from bimolecular reactions because of the interference of diffusion.[152−154] Particularly, for e_{aq}^- reactions, only one system has been reported that reveals the rate decrease in the inverted region.[155] The e_{aq}^- reaction with $Ru(bpy)_3^{3+}$ to form the ground state of $Ru(bpy)_3^{2+}$ has $\Delta G = -4.14$ eV, but the reaction can also form the charge-transfer excited state with $\Delta G = -2.03$ eV. The rate constant of the former reaction has been found to be $\sim 3 \times 10^9$ M^{-1} s^{-1}, at most, at room temperature, while the latter reaction has a rate constant of 2.0×10^{10} M^{-1} s^{-1}.

Arguments against the possibility of the contribution of k_{act} to k_{obs} can be made by observing the behavior of the e_{aq}^- reactions with nitrobenzene ($C_6H_5NO_2$) and methylviologen dication (MV^{2+}) over a wide range of temperature, 20 to >200 °C.[93,126] Both reactions are highly exoergic ($\Delta G = -2.38$ and -2.43 eV, respectively). The observed rate constants have been analyzed with the Smoluchowski equation, and diffusion control of the reactions is maintained, even at high temperatures, with the observed rate constant of $\sim 1 \times 10^{12}$ M^{-1} s^{-1}. Apparently, the true rate constants for these reactions are much higher than this value. If the e_{aq}^- + radical reactions in our study have similarly large intrinsic rate constants, then they will not affect the observed rate constants. It should also be mentioned that there appear to be little correlation between k_{obs} and ΔG (Table 7).

The final products of the e_{aq}^- reactions with the dihalogen radical anions are the corresponding halide anions. However, simple electron transfer leads to an intermediate state before the final products are formed.

$$e_{aq}^- + X_2^{\bullet-} \leftrightarrow X_2^{2-} \rightarrow 2X^- \qquad (10)$$

It has been reported that formation of intermediate states affects the temperature dependence of the e_{aq}^- reactions with NO_2^-, NO_3^-, and N_2O.[93] The Arrhenius plots of the rate constants for these reactions curve down toward higher temperatures, presumably as a result of the equilibrium between the reactants and the corresponding intermediate states. This mechanism may influence the apparent activation energies for the e_{aq}^- reactions with $Br_2^{\bullet-}$ and $I_2^{\bullet-}$. It should be remembered, however, that very large observed rate constants for the two reactions suggest that such an equilibrium (eq 10) would not affect the observed rate constant very much, at least at room temperature.

Homogeneous versus Geminate Reactions. Recent experimental studies of ultrafast dynamics following photodetachment/photoionization in aqueous solution have addressed questions pertaining to kinetics of geminate e_{aq}^-/radical pairs. In this section, comments will be made on comparison of geminate dynamics and homogeneous e_{aq}^- + radical reactions.

Bradforth and co-workers have studied geminate reaction between e_{aq}^- and $^{\bullet}OH$ following photodetachment of the hydroxide anion (OH^-).[39,42] For the kinetic analysis, they adopted a model that assumes a weak mutual interaction between the two reactants. After the geminate pair is formed in the shallow potential well, the two reactants can either react to form the parent OH^- or escape diffusively. This kinetic analysis allowed them to derive an effective reaction radius of 5.6 Å for the e_{aq}^-−$^{\bullet}OH$ geminate reaction. Then they compared this value with an effective reaction radius for the homogeneous e_{aq}^- + $^{\bullet}OH$ reaction derived from eq 1 using a spin factor of 1, and mentioned that there is good agreement between the two values. Furthermore, from the geminate kinetic analysis over a temperature range of 8−97 °C, they found that the effective reaction distance for the geminate reaction is independent of temperature. On the basis of these observations, they concluded that the homogeneous e_{aq}^- + $^{\bullet}OH$ reaction is diffusion-controlled, and they questioned the low activation energy found by Elliot and Ouellette[23] for the bulk reaction.

While we certainly recognize a logical point in their comparison of geminate and homogeneous kinetics, we note a few counter arguments. They adopted a geminate kinetic model, based on Shushin's formulation,[156−158] where the two reactants feel a weak, but significant, mutual interaction. Without such an interaction, they were unable to fit the time dependence of the e_{aq}^- survival probability.[39] In earlier attempts to fit the geminate dynamics following photodetachment from OH^- and I^-, solutions of the diffusion equations were sought only with either the absorbing boundary condition or the radiation boundary condition.[35,39] It is questionable whether or not a genuine physical picture of the geminate system can be reproduced when the dependence of the reaction probability on the reaction coordinates is ignored. It is well recognized that difficulties in solving the diffusion equations arise when specific forms of reaction probability as a function of reaction coordinates have to be taken into account.[132,159,160] In the model that takes account of the mutual interaction, the effects of the distance dependence of the reaction probability could be folded in the rate constant for the geminate pairs within the potential well to some extent. However, it is uncertain how the effects of long-range electron-transfer reaction are reflected in the parameters of such a model. Another point, which is obvious and probably important, is complete neglect of spin dynamics in their analysis.

They have also studied photodetachment from sulfite ion (SO_3^{2-}) in aqueous solution.[38,42] Unlike the e_{aq}^-/$^{\bullet}OH$ geminate pair, the e_{aq}^-/$^{\bullet}SO_3^-$ geminate pair does not experience efficient fast decay on the order of 10 ps, indicative of rather large initial separations of the two radicals. The absence of fast decay completely precludes comparison of the geminate and homogeneous kinetics. The present study of the e_{aq}^- + $^{\bullet}SO_3^-$ reaction indicates that the homogeneous reaction is diffusion-controlled with a spin factor of $^1/_4$.

It is interesting to consider the ultrafast dynamics of photoionization of indole at this point. Kohler and co-workers found no decay of geminate e_{aq}^-/indole radical cation pair up to 100 ps after a monophotonic photoionization event induced by a femtosecond laser pulse (260 nm).[30] This result is consistent with an earlier study by Mialocq et al. who used a picosecond laser.[161] They concluded that the reaction rate between e_{aq}^- and the indole radical cation is rather slow such that it would not be diffusion-limited if they random-encountered. This proposition seems at odds with the results of the present study. The reduction potential of the indole radical cation has been reported to be +1.24 V,[162,163] and the magnitude of ΔG for this reaction is not larger than those for a number of e_{aq}^- reactions studied

in this paper. Thus, on the basis of our study, the e_{aq}^- reaction with the indole radical cation would be most likely to be diffusion-controlled. Unlike photodetachment from polyvalent anions[42] such as SO_3^{2-} and $Fe(CN)_6^{4-}$, the mutual interaction in the geminate pair is not repulsive but attractive in the photoionization of indole. It is not clear whether the initial separations of the two radicals could be large enough to suppress efficient geminate recombination following the monophotonic ionization of indole in aqueous solution.

Conclusion

The rate constants of e_{aq}^- reactions with various reactive radicals have been measured over a temperature range of 5−75 °C using the pulse radiolysis technique. This work considerably expands the knowledge of e_{aq}^- + radical reaction rates. It has been concluded that many radicals react with e_{aq}^- in a diffusion-controlled manner with a reaction distance of 5−10 Å and a spin factor of $^1/_4$ based on the Smoluchowski analysis. Spin factors of much larger than $^1/_4$ have been assigned for the e_{aq}^- reactions with $^\bullet OH$, $^\bullet N_3$, $Br_2^{\bullet-}$, $I_2^{\bullet-}$, and $C_6H_5S^\bullet$ at room temperature. Such large spin factors can result from fast singlet−triplet conversion during the radical encounter. The large spin factors for the $^\bullet OH$, $^\bullet N_3$, and $C_6H_5S^\bullet$ reactions have been ascribed to their fast spin relaxation. The spin relaxation of these radicals is likely to be related to the spin−orbit coupling for nearly degenerate orbitals. In the case of $Br_2^{\bullet-}$ and $I_2^{\bullet-}$, it is most probable that singlet−triplet conversion for the $e_{aq}^-/Br_2^{\bullet-}$ or $I_2^{\bullet-}$ pair takes place by the heavy-atom-spin−orbit effect. The temperature dependence of the rate constants of these reactions suggests that the spin factor decreases with temperature as a result of competition between diffusion and singlet−triplet conversion in the radical pair.

The present kinetic study provides further experimental data to help understand the CIDEP behavior observed for many e_{aq}^-/radical pairs. Inverted CIDEP has been reported for the random encounter pairs of e_{aq}^- with $C_6H_5O^\bullet$, $CO_3^{\bullet-}$, and p-$OC_6H_4O^{\bullet-}$, while normal CIDEP has been reported for those with $^\bullet SO_3^-$, $^\bullet CO_2^-$, and $(^\bullet CH_2)(CH_3)_2COH$.[3] The spin multiplicity of the random encounter pairs must be the same for the two groups (i.e., triplet because singlet pairs are quenched by reaction). Therefore, the energy ordering of the radical pair states must be different between the two groups. The reversal of the energy ordering has been discussed[6] in terms of electronic interaction between the radical pair states and the reaction product states at the equilibrium configuration of the radical pairs, following the arguments of Kobori et al.[8−10]

Acknowledgment. This work was supported by the Office of Basic Energy Science of the U.S. Department of Energy. This is contribution no. NDRL-4699 from the Notre Dame Radiation Laboratory. The authors thank Dr. N. J. B. Green for a number of helpful discussions. Also, we thank the reviewers for useful suggestions.

Supporting Information Available: PDF file containing (1) text detailing the analysis method for the e_{aq}^- + secondary radical reactions; (2) text explaining reorganization energies for the e_{aq}^- + radical reactions; (3) Table S1: data of the rate constants of the self-reactions of the secondary radicals; (4) Table S2: data of the rate constants of the e_{aq}^- + I_2 reaction; (5) Table S3: data of the rate constants of the e_{aq}^- + secondary radical reactions; (6) Figure S1: Arrhenius plots for the rate constants of the self-reactions of the alcohol radicals. This material is available free of charge via the Internet at http://pubs.acs.org.

References and Notes

(1) Pedersen, J. B.; Freed, J. H. *J. Chem. Phys.* **1973**, *58*, 2746−2762.
(2) McLauchlan, K. A. Continuous-Wave Transient Electron Spin Resonance. In *Modern Pulsed and Continuous-Wave Electron Spin Resonance*; Kevan, L., Bowman, M. K., Eds.; John Wiley & Sons: New York, 1990.
(3) Fessenden, R. W.; Verma, N. C. *J. Am. Chem. Soc.* **1976**, *98*, 243−244.
(4) Jeevarajan, A. S.; Fessenden, R. W. *J. Phys. Chem.* **1992**, *96*, 1520−1523.
(5) Ichino, T. On the Mechanism of Unusual CIDEP. Ph.D. Dissertation, University of Notre Dame, Notre Dame, IN, 2001.
(6) Ichino, T.; Fessenden, R. W. *J. Phys. Chem. A* **2003**, *107*, 9257−9268.
(7) Bussandri, A.; van Willigen, H. *J. Phys. Chem. A* **2001**, *105*, 4669−4675.
(8) Sekiguchi, S.; Kobori, Y.; Akiyama, K.; Tero-Kubota, S. *J. Am. Chem. Soc.* **1998**, *120*, 1325−1326.
(9) Kobori, Y.; Sekiguchi, S.; Akiyama, K.; Tero-Kubota, S. *J. Phys. Chem. A* **1999**, *103*, 5416−5424.
(10) Kobori, Y.; Akiyama, K.; Tero-Kubota, S. *J. Chem. Phys.* **2000**, *113*, 465−468.
(11) Marcus, R. A. *J. Chem. Phys.* **1956**, *24*, 966−978.
(12) Hush, N. S. *Trans. Faraday Soc.* **1961**, *57*, 557−580.
(13) Hart, E. J.; Anbar, M. *The Hydrated Electron*; Wiley-Interscience: New York, 1970.
(14) Schwarz, H. A. *J. Chem. Educ.* **1981**, *58*, 101−105.
(15) Han, P.; Bartels, D. M. *J. Phys. Chem.* **1990**, *94*, 7294−7299.
(16) Lind, J.; Shen, X.; Eriksen, T. E.; Merenyi, G. *J. Am. Chem. Soc.* **1990**, *112*, 479−482.
(17) Hyperfine interaction (as well as, in the presence of magnetic field, the Larmor frequency difference) can induce singlet−triplet conversion for radical pairs between an encounter and any subsequent re-encounters, which modifies the spin factor for singlet reaction. For the radical systems in the present study, this transition may raise the statistical factor from 0.25 by, perhaps, up to 0.02; see Figure 8b in ref 1. We ignore such an effect and continue to use the nominal value for discussion.
(18) Buxton, G. V.; Greenstock, C. L.; Helman, W. P.; Ross, A. B. *J. Phys. Chem. Ref. Data* **1988**, *17*, 513−886.
(19) The Radiation Chemistry Data Center, Notre Dame Radiation Laboratory, http://allen.rad.nd.edu.
(20) Buxton, G. V. Radiation Chemistry of the Liquid State: (1) Water and Homogeneous Aqueous Solutions. In *Radiation Chemistry: Principles and Applications*; Farhataziz, Rodgers, A. J., Eds.; VCH: New York, 1987; Chapter 10.
(21) Matheson, M. S.; Rabani, J. *J. Phys. Chem.* **1965**, *69*, 1324−1335.
(22) Christensen, H.; Sehested, K.; Logager, T. *Radiat. Phys. Chem.* **1994**, *43*, 527−531.
(23) Elliot, A. J.; Ouellette, D. C. *J. Chem. Soc., Faraday Trans.* **1994**, *90*, 837−841.
(24) Gauduel, Y.; Pommeret, S.; Migus, A.; Antonetti, A. *J. Phys. Chem.* **1989**, *93*, 3880−3882.
(25) Gauduel, Y.; Pommeret, S.; Migus, A.; Antonetti, A. *J. Phys. Chem.* **1991**, *95*, 533−539.
(26) Crowell, R. A.; Bartels, D. M. *J. Phys. Chem.* **1996**, *100*, 17713−17715.
(27) Crowell, R. A.; Bartels, D. M. *J. Phys. Chem.* **1996**, *100*, 17940−17949.
(28) Kloepfer, J. A.; Vilchiz, V. H.; Lenchenkov, V. A.; Bradforth, S. E. *Chem. Phys. Lett.* **1998**, *298*, 120−128.
(29) Thomsen, C. L.; Madsen, D.; Keiding, S. R.; Thogersen, J.; Christiansen, O. *J. Chem. Phys.* **1999**, *110*, 3453−3462.
(30) Peon, J.; Hess, G. C.; Pecourt, J. M. L.; Yuzawa, T.; Kohler, B. *J. Phys. Chem. A* **1999**, *103*, 2460−2466.
(31) Kloepfer, J. A.; Vilchiz, V. H.; Lenchenkov, V. A.; Germaine, A. C.; Bradforth, S. E. *J. Chem. Phys.* **2000**, *113*, 6288−6307.
(32) Madsen, D.; Thomsen, C. L.; Thogersen, J.; Keiding, S. R. *J. Chem. Phys.* **2000**, *113*, 1126−1134.
(33) Vilchiz, V. H.; Kloepfer, J. A.; Germaine, A. C.; Lenchenkov, V. A.; Bradforth, S. E. *J. Phys. Chem. A* **2001**, *105*, 1711−1723.
(34) Pommeret, S.; Gobert, F.; Mostafavi, A.; Lampre, I.; Mialocq, J. C. *J. Phys. Chem. A* **2001**, *105*, 11400−11406.
(35) Kloepfer, J. A.; Vilchiz, V. H.; Lenchenkov, V. A.; Chen, X. Y.; Bradforth, S. E. *J. Chem. Phys.* **2002**, *117*, 766−778.
(36) Sauer, M. C.; Crowell, R. A.; Shkrob, I. A. *J. Phys. Chem. A* **2004**, *108*, 5490−5502.
(37) Crowell, R. A.; Lian, R.; Shkrob, I. A.; Qian, J.; Oulianov, D. A.; Pommeret, S. *J. Phys. Chem. A* **2004**, *108*, 9105−9114.

(38) Sauer, M. C.; Shkrob, I. A.; Lian, R.; Crowell, R. A.; Bartels, D. M.; Chen, X. Y.; Suffern, D.; Bradforth, S. E. *J. Phys. Chem. A* **2004**, *108*, 10414−10425.
(39) Crowell, R. A.; Lian, R.; Shkrob, I. A.; Bartels, D. M.; Chen, X. Y.; Bradforth, S. E. *J. Chem. Phys.* **2004**, *120*, 11712−11725.
(40) Lian, R.; Crowell, R. A.; Shkrob, I. A.; Bartels, D. M.; Oulianov, D. A.; Gosztola, D. *Chem. Phys. Lett.* **2004**, *389*, 379−384.
(41) Lian, R.; Oulianov, D. A.; Shkrob, I. A.; Crowell, R. A. *Chem. Phys. Lett.* **2004**, *398*, 102−106.
(42) Lian, R.; Oulianov, D. A.; Crowell, R. A.; Shkrob, I. A.; Chen, X. Y.; Bradforth, S. E. *J. Phys. Chem. A* **2006**, *110*, 9071−9078.
(43) Elles, C. G.; Jailaubekov, A. E.; Crowell, R. A.; Bradforth, S. E. *J. Chem. Phys.* **2006**, *125*, 044515.
(44) Pimblott, S. M.; LaVerne, J. A.; Bartels, D. M.; Jonah, C. D. *J. Phys. Chem.* **1996**, *100*, 9412−9415.
(45) Bartels, D. M.; Cook, A. R.; Mudaliar, M.; Jonah, C. D. *J. Phys. Chem. A* **2000**, *104*, 1686−1691.
(46) Bartels, D. M.; Gosztola, D.; Jonah, C. D. *J. Phys. Chem. A* **2001**, *105*, 8069−8072.
(47) Rice, S. A. *Diffusion-Limited Reactions*; Elsevier: Amsterdam, 1985.
(48) Salikhov, K. M.; Molin, Y. N.; Sagdeev, R. Z.; Buchachenko, A. L. *Spin Polarization and Magnetic Effects in Radical Reactions*; Elsevier: Amsterdam, 1984.
(49) Burshtein, A. I.; Khudyakov, I. V.; Yakobson, B. I. *Prog. React. Kinet.* **1984**, *13*, 221−305.
(50) Fischer, H.; Paul, H. *Acc. Chem. Res.* **1987**, *20*, 200−206.
(51) Saltiel, J.; Atwater, B. W. Spin-Statistical Factors in Diffusion-Controlled Reactions. In *Advances in Photochemistry*; Volman, D. H., Hammond, G. S., Gollnick, K., Eds.; John Wiley and Sons: New York, 1988; Vol. 14; pp 1−90.
(52) Buxton, G. V.; Elliot, A. J. *J. Chem. Soc., Faraday Trans.* **1993**, *89*, 485−488.
(53) Whitham, K.; Lyons, S.; Miller, R.; Nett, D.; Treas, P.; Zante, A.; Fessenden, R. W.; Thomas, M. D.; Wang, Y. *Proc. Part. Accel. Conf., 16th, 1995*, **1996**, 131−133.
(54) Hug, G. L.; Wang, Y. C.; Schoneich, C.; Jiang, P. Y.; Fessenden, R. W. *Radiat. Phys. Chem.* **1999**, *54*, 559−566.
(55) Mezyk, S. P.; Madden, K. P. *J. Phys. Chem. A* **1999**, *103*, 235−242.
(56) Schuler, R. H.; Patterson, L. K.; Janata, E. *J. Phys. Chem.* **1980**, *84*, 2088−2089.
(57) Buxton, G. V.; Stuart, C. R. *J. Chem. Soc., Faraday Trans.* **1995**, *91*, 279−281.
(58) LaVerne, J. A.; Pimblott, S. M. *J. Chem. Soc., Faraday Trans.* **1993**, *89*, 3527−3532.
(59) There is a significant difference in the $G\epsilon$ values for the thiocyanate system reported in refs 56 and 57. We take a value from ref 57 because the study apparently used a more careful approach to deterimine the $G\epsilon$ values.
(60) Christensen, H.; Sehested, K. *J. Phys. Chem.* **1986**, *90*, 186−190.
(61) Bartels, D. M.; Takahashi, K.; Cline, J. A.; Marin, T. W.; Jonah, C. D. *J. Phys. Chem. A* **2005**, *109*, 1299−1307.
(62) Elliot, A. J.; Chenier, M. P.; Ouellette, D. C. *J. Chem. Soc., Faraday Trans.* **1993**, *89*, 1193−1197.
(63) Throughout this paper, an activation energy determined from an Arrhenius plot of observed rate constants (k_{obs} or k_0) is called an apparent activation energy. An activation energy determined from an Arrhenius plot of true rate constants (k_{act}) is called a true activation energy.
(64) Press, W. H.; Teukolsky, S. A.; Vetterling, W. T.; Flannery, B. P. *Numerical Recipes*, 2nd ed.; Cambridge University Press: Cambridge, 1992.
(65) Perrin, D. D. *Ionization Constants of Inorganic Acids and Bases in Aqueous Solution*; Pergamon Press: New York, 1982.
(66) Mesmer, R. E.; Baes, C. F., Jr.; Sweeton, F. H. *Inorg. Chem.* **1972**, *11*, 537−543.
(67) Farrington, J. A.; Ebert, M.; Land, E. J. *J. Chem. Soc., Faraday Trans. 1* **1978**, *74*, 665−675.
(68) Gordon, S.; Schmidt, K. H.; Hart, E. J. *J. Phys. Chem.* **1977**, *81*, 104−109.
(69) Fojtik, A.; Czapski, G.; Henglein, A. *J. Phys. Chem.* **1970**, *74*, 3204−3208.
(70) Schmidt, K. H.; Han, P.; Bartels, D. M. *J. Phys. Chem.* **1992**, *96*, 199−206.
(71) Schmidt, K. H.; Han, P.; Bartels, D. M. *J. Phys. Chem.* **1995**, *99*, 10530−10539.
(72) Busi, F.; D'Angelantonio, M.; Bettoli, G.; Concialini, V.; Tubertini, O.; Barker, G. C. *Inorg. Chim. Acta* **1984**, *84*, 105−111.
(73) Schwarz, H. A.; Gill, P. S. *J. Phys. Chem.* **1977**, *81*, 22−25.
(74) Benson, S. W. *The Foundations of Chemical Kinetics*; McGraw-Hill: New York, 1960.
(75) McQuarrie, D. A. *Statistical Mechanics*; Harper Collins: New York, 1976.
(76) Chawla, O. P.; Fessenden, R. W. *J. Phys. Chem.* **1975**, *79*, 2693−2700.
(77) Atkins, P. W.; Symons, M. C. R. *The Structure of Inorganic Radicals*; Elsevier: Amsterdam, 1967.
(78) Verma, N. C.; Fessenden, R. W. *J. Chem. Phys.* **1976**, *65*, 2139−2155.
(79) Brivati, J. A.; Symons, M. C. R.; Tinling, D. J. A.; Wardale, H. W.; Williams, D. O. *Chem. Commun.* **1965**, 402−403.
(80) Dibdin, G. H. *Trans. Faraday Soc.* **1967**, *63*, 2098−2111.
(81) Brivati, J. A.; Symons, M. C. R.; Tinling, D. J. A.; Wardale, H. W.; Williams, D. O. *Trans. Faraday Soc.* **1967**, *63*, 2112−2116.
(82) Riederer, H.; Huttermann, J.; Boon, P.; Symons, M. C. R. *J. Magn. Reson.* **1983**, *54*, 54−66.
(83) Langford, V. S.; McKinley, A. J.; Quickenden, T. I. *J. Am. Chem. Soc.* **2000**, *122*, 12859−12863.
(84) Cooper, P. D.; Kjaergaard, H. G.; Langford, V. S.; McKinley, A. J.; Quickenden, T. I.; Schofield, D. P. *J. Am. Chem. Soc.* **2003**, *125*, 6048−6049.
(85) Ohshima, Y.; Sato, K.; Sumiyoshi, Y.; Endo, Y. *J. Am. Chem. Soc.* **2005**, *127*, 1108−1109.
(86) Brauer, C. S.; Sedo, G.; Grumstrup, E. M.; Leopold, K. R.; Marshall, M. D.; Leung, H. O. *Chem. Phys. Lett.* **2005**, *401*, 420−425.
(87) Marshall, M. D.; Lester, M. I. *J. Phys. Chem. B* **2005**, *109*, 8400−8406.
(88) Winter, G.; Shioyama, H.; Steiner, U. *Chem. Phys. Lett.* **1981**, *81*, 547−552.
(89) The spin-rotation mechanism is probably very effective for the spin relaxation of nitrite radical because of the small moment of inertia. See Behar, D.; Fessenden, R. W. *J. Phys. Chem.* **1972**, *76*, 1706, and ref 76. However, it is likely that the spin relaxation of nitrite radical is not as fast as that of the azidyl radical.
(90) Treinin, A.; Loeff, I.; Hurley, J. K.; Linschitz, H. *Chem. Phys. Lett.* **1983**, *95*, 333−338.
(91) Hurley, J. K.; Linschitz, H.; Treinin, A. *J. Phys. Chem.* **1988**, *92*, 5151−5159.
(92) Claxton, T. A.; Overill, R. E.; Symons, M. C. R. *Mol. Phys.* **1973**, *26*, 75−80.
(93) Elliot, A. J.; McCracken, D. R.; Buxton, G. V.; Wood, N. D. *J. Chem. Soc., Faraday Trans.* **1990**, *86*, 1539−1547.
(94) Tripathi, G. N. R.; Schuler, R. H. *J. Chem. Phys.* **1984**, *81*, 113−121.
(95) Tripathi, G. N. R.; Sun, Q.; Armstrong, D. A.; Chipman, D. M.; Schuler, R. H. *J. Phys. Chem.* **1992**, *96*, 5344−5350.
(96) Chipman, D. M.; Liu, R.; Zhou, X.; Pulay, P. *J. Chem. Phys.* **1994**, *100*, 5023−5035.
(97) Becconsall, J. K.; Clough, S.; Scott, G. *Trans. Faraday Soc.* **1960**, *56*, 459−472.
(98) Dixon, W. T.; Moghimi, M.; Murphy, D. *J. Chem. Soc., Faraday Trans. 2* **1974**, *70*, 1713−1720.
(99) Schuler, R. H.; Neta, P.; Zemel, H.; Fessenden, R. W. *J. Am. Chem. Soc.* **1976**, *98*, 3825−3831.
(100) Batchelor, S. N.; Kay, C. W. M.; McLauchlan, K. A.; Yeung, M. T. *J. Phys. Chem.* **1993**, *97*, 4570−4572.
(101) Zandstra, P. J.; Michaelsen, J. D. *J. Chem. Phys.* **1963**, *39*, 933−938.
(102) Schmidt, U.; Mueller, A. *Angew. Chem., Int. Ed.* **1963**, *2*, 216.
(103) Schmidt, U. *Angew. Chem., Int. Ed.* **1964**, *3*, 602−608.
(104) Schmidt, U.; Mueller, A.; Markau, K. *Chem. Ber.* **1964**, *97*, 405−414.
(105) Morke, W.; Jezierski, A.; Singer, H. *Z. Chem.* **1979**, *19*, 147−148.
(106) Jeschke, G.; Wakasa, M.; Sakaguchi, Y.; Hayashi, H. *J. Phys. Chem.* **1994**, *98*, 4069−4075.
(107) Hayashi, H.; Nagakura, S. *Bull. Chem. Soc. Jpn.* **1978**, *51*, 2862−2866.
(108) Hayashi, H.; Nagakura, S. *Bull. Chem. Soc. Jpn.* **1984**, *57*, 322−328.
(109) Carrington, A.; McLachlan, A. D. *Introduction to Magnetic Resonance*; Harper and Row: New York, 1967.
(110) Marov, I.; Symons, M. C. R. *J. Chem. Soc. A* **1971**, 201−204.
(111) McLauchlan, K. A.; Sealy, R. C.; Wittmann, J. M. *Mol. Phys.* **1978**, *36*, 1397−1407.
(112) Steiner, U.; Winter, G. *Chem. Phys. Lett.* **1978**, *55*, 364−368.
(113) Steiner, U. *Ber. Bunsen-Ges. Phys. Chem.* **1981**, *85*, 228−233.
(114) Ulrich, T.; Steiner, U. E.; Foll, R. E. *J. Phys. Chem.* **1983**, *87*, 1873−1882.
(115) Kikuchi, K.; Hoshi, M.; Abe, E.; Kokubun, H. *J. Photochem. Photobiol. A* **1988**, *45*, 1−7.
(116) Kikuchi, K.; Hoshi, M.; Niwa, T.; Takahashi, Y.; Miyashi, T. *J. Phys. Chem.* **1991**, *95*, 38−42.
(117) Steiner, U. E.; Haas, W. *J. Phys. Chem.* **1991**, *95*, 1880−1890.
(118) Katsuki, A.; Akiyama, K.; Ikegami, Y.; Tero-Kubota, S. *J. Am. Chem. Soc.* **1994**, *116*, 12065−12066.
(119) Katsuki, A.; Akiyama, K.; Tero-Kubota, S. *Bull. Chem. Soc. Jpn.* **1995**, *68*, 3383−3389.

(120) Kleverlaan, C. J.; Martino, D. M.; van Willigen, H.; Stufkens, D. J.; Oskam, A. *J. Phys. Chem.* **1996**, *100*, 18607−18611.
(121) Sasaki, S.; Katsuki, A.; Akiyama, K.; Tero-Kubota, S. *J. Am. Chem. Soc.* **1997**, *119*, 1323−1327.
(122) Sasaki, S.; Kobori, Y.; Akiyama, K.; Tero-Kubota, S. *J. Phys. Chem. A* **1998**, *102*, 8078−8083.
(123) Ferraudi, G. *J. Phys. Chem.* **1993**, *97*, 2793−2797.
(124) Mints, R. G.; Pukhov, A. A. *Chem. Phys.* **1984**, *87*, 467−472.
(125) $T_1 = T_2$ is assumed.
(126) Marin, T. W.; Cline, J. A.; Takahashi, K.; Bartels, D. M.; Jonah, C. D. *J. Phys. Chem. A* **2002**, *106*, 12270−12279.
(127) Maham, Y.; Freeman, G. R. *Can. J. Chem.* **1988**, *66*, 1706−1711.
(128) Cannon, R. D. *Electron Transfer Reactions*; Butterworths: London, 1980.
(129) Doktorov, A. B.; Burshtein, A. I. *Sov. Phys. JETP* **1975**, *41*, 671−677.
(130) Pilling, M. J.; Rice, S. A. *J. Chem. Soc., Faraday Trans. 2* **1975**, *71*, 1563−1571.
(131) According to ref 73, the reaction distance of the e_{aq}^- reaction with I_2 is 11 Å at room temperature. We show in the Supporting Information that the apparent activation energy of this reaction is 17.3 ± 0.6 kJ mol^{-1} over a temperature range of 20−70 °C. Thus, analogous to the e_{aq}^- + nitrobenzene reaction system, the reaction distance may decrease with temperature in this system.
(132) Gladkikh, V. S.; Burshtein, A. I.; Tavernier, H. L.; Fayer, M. D. *J. Phys. Chem. A* **2002**, *106*, 6982−6990.
(133) Burshtein, A. I.; Frantsuzov, P. A. *J. Lumin.* **1992**, *51*, 215−222.
(134) Wolff, H. J.; Burssner, D.; Steiner, U. E. *Pure Appl. Chem.* **1995**, *67*, 167−174.
(135) Burshtein, A. I.; Krissinel, E. *J. Phys. Chem. A* **1998**, *102*, 816−824.
(136) The analysis of the stochastic Liouville equation for CIDEP in ref 1 essentially gives the same conclusion.
(137) Lukzen, N. N.; Pedersen, J. B.; Burshtein, A. I. *J. Phys. Chem. A* **2005**, *109*, 11914−11926.
(138) Gladkikh, V. S.; Burshtein, A. I. *Chem. Phys.* **2006**, *323*, 351−357.
(139) Gladkikh, V. S.; Burshtein, A. I. *J. Phys. Chem. A* **2006**, *110*, 3364−3376.
(140) Ichino, T.; Fessenden, R. W. unpublished data.
(141) Armstrong, D. A.; Sun, Q.; Schuler, R. H. *J. Phys. Chem.* **1996**, *100*, 9892−9899.
(142) Benderskii, V. A.; Krivenko, A. G.; Rukin, A. N. *Khim. Vys. Energ.* **1980**, *14*, 400−405.
(143) Benderskii, V. A.; Krivenko, A. G. *Elektrokhimiya* **1996**, *32*, 721−727.
(144) Fessenden, R. W.; Hornak, J. P.; Venkataraman, B. *J. Chem. Phys.* **1981**, *74*, 3694−3704.
(145) Schmidt, K. H.; Bartels, D. M. *Chem. Phys.* **1995**, *190*, 145−152.
(146) In ref 71, the zero-field splitting mixing of the doublet−quartet pair states has been considered. In addition, the spin relaxation time for O_2 must be very short due to the modulation of the zero-field splitting.
(147) Miller, J. R.; Calcaterra, L. T.; Closs, G. L. *J. Am. Chem. Soc.* **1984**, *106*, 3047−3049.
(148) Closs, G. L.; Miller, J. R. *Science* **1988**, *240*, 440−447.
(149) Barbara, P. F.; Meyer, T. J.; Ratner, M. A. *J. Phys. Chem.* **1996**, *100*, 13148−13168.
(150) Liang, N.; Miller, J. R.; Closs, G. L. *J. Am. Chem. Soc.* **1990**, *112*, 5353−5354.
(151) Kroon, J.; Oevering, H.; Verhoeven, J. W.; Warman, J. M.; Oliver, A. M.; Paddon-Row, M. N. *J. Phys. Chem.* **1993**, *97*, 5065−5069.
(152) Rehm, D.; Weller, A. *Isr. J. Chem.* **1970**, *8*, 259.
(153) Turro, C.; Zaleski, J. M.; Karabatsos, Y. M.; Nocera, D. G. *J. Am. Chem. Soc.* **1996**, *118*, 6060−6067.
(154) Guldi, D. M.; Luo, C.; Prato, M.; Dietel, E.; Hirsch, A. *Chem. Commun.* **2000**, 373−374.
(155) Jonah, C. D.; Matheson, M. S.; Meisel, D. *J. Am. Chem. Soc.* **1978**, *100*, 1449−1456.
(156) Shushin, A. I. *Chem. Phys. Lett.* **1985**, *118*, 197−202.
(157) Shushin, A. I. *J. Chem. Phys.* **1991**, *95*, 3657−3665.
(158) Shushin, A. I. *J. Chem. Phys.* **1992**, *97*, 1954−1960.
(159) Burshtein, A. I. *Adv. Chem. Phys.* **2000**, *114*, 419−587.
(160) Gladkikh, V.; Burshtein, A. I.; Angulo, G.; Pages, S.; Lang, B.; Vauthey, E. *J. Phys. Chem. A* **2004**, *108*, 6667−6678.
(161) Mialocq, J. C.; Amouyal, E.; Bernas, A.; Grand, D. *J. Phys. Chem.* **1982**, *86*, 3173−3177.
(162) Merenyi, G.; Lind, J.; Shen, X. *J. Phys. Chem.* **1988**, *92*, 134−137.
(163) Jovanovic, S. V.; Steenken, S. *J. Phys. Chem.* **1992**, *96*, 6674−6679.
(164) Christensen, H.; Sehested, K.; Corfitzen, H. *J. Phys. Chem.* **1982**, *86*, 1588−1590.
(165) Christensen, H.; Sehested, K. *J. Phys. Chem.* **1983**, *87*, 118−120.
(166) Sehested, K.; Christensen, H. *Radiat. Phys. Chem.* **1990**, *36*, 499−500.
(167) Han, P.; Bartels, D. M. *J. Phys. Chem.* **1992**, *96*, 4899−4906.
(168) Mezyk, S. P.; Bartels, D. M. *J. Chem. Soc., Faraday Trans.* **1995**, *91*, 3127−3132.
(169) Elliot, A. J.; Simsons, A. S. *Radiat. Phys. Chem.* **1984**, *24*, 229−231.
(170) Mezyk, S. P.; Bartels, D. M. *J. Phys. Chem. A* **1997**, *101*, 1329−1333.
(171) Huie, R. E.; Neta, P. *Atmos. Environ.* **1987**, *21*, 1743−1747.
(172) Buxton, G. V.; Wood, N. D.; Dyster, S. *J. Chem. Soc., Faraday Trans. 1* **1988**, *84*, 1113−1121.
(173) Ashton, L.; Buxton, G. V.; Stuart, C. R. *J. Chem. Soc., Faraday Trans.* **1995**, *91*, 1631−1633.
(174) Roduner, E.; Bartels, D. M. *Ber. Bunsen-Ges. Phys. Chem.* **1992**, *96*, 1037−1042.
(175) Alfassi, Z. B.; Schuler, R. H. *J. Phys. Chem.* **1985**, *89*, 3359−3363.
(176) Ye, M.; Madden, K. P.; Fessenden, R. W.; Schuler, R. H. *J. Phys. Chem.* **1986**, *90*, 5397−5399.
(177) Alfassi, Z. B.; Huie, R. E.; Neta, P.; Shoute, L. C. T. *J. Phys. Chem.* **1990**, *94*, 8800−8805.
(178) Gary-Bobo, C. M.; Weber, H. W. *J. Phys. Chem.* **1969**, *73*, 1155−1156.
(179) Pratt, K. C.; Wakeham, W. A. *Proc. R. Soc. London, Ser. A* **1975**, *342*, 401−419.
(180) *CRC Handbook of Chemistry and Physics*, 77th ed.; CRC: Boca Raton, FL, 1996.
(181) Bonoli, L.; Witherspoon, P. A. *J. Phys. Chem.* **1968**, *72*, 2532−2534.
(182) Tominaga, T.; Yamamoto, S.; Tanaka, J. *J. Chem. Soc., Faraday Trans. 1* **1984**, *80*, 941−947.
(183) Robinson, R. A.; Stokes, R. H. *Electrolyte Solutions*, 2nd ed.; Butterworths: London, 1965.
(184) Witherspoon, P. A.; Saraf, D. N. *J. Phys. Chem.* **1965**, *69*, 3752−3755.
(185) Biondi, C.; Bellugi, L. *Chem. Phys.* **1981**, *62*, 145−152.
(186) Rossky, P. J.; Schnitker, J. *J. Phys. Chem.* **1988**, *92*, 4277−4285.
(187) Friedman, M. E.; Scheraga, H. A. *J. Phys. Chem.* **1965**, *69*, 3795−3800.
(188) Bondi, A. *J. Phys. Chem.* **1964**, *68*, 441−451.
(189) Edward, J. T. *J. Chem. Educ.* **1970**, *47*, 261−270.
(190) Jenkins, H. D. B.; Thakur, K. P. *J. Chem. Educ.* **1979**, *56*, 576−577.
(191) Wells, A. F. *Structural Inorganic Chemistry*, 5th ed.; Oxford University Press: New York, 1984.
(192) Masterton, W. L. *J. Chem. Phys.* **1954**, *22*, 1830−1833.
(193) Jeevarajan, A. S.; Fessenden, R. W. *J. Phys. Chem.* **1989**, *93*, 3511−3514.
(194) Bartels, D. M.; Lawler, R. G.; Trifunac, A. D. *J. Chem. Phys.* **1985**, *83*, 2686−2707.
(195) Dixon, W. T.; Norman, R. O. C. *J. Chem. Soc.* **1963**, 3119−3124.
(196) Livingston, R.; Zeldes, H. *J. Am. Chem. Soc.* **1966**, *88*, 4333−4336.
(197) Eiben, K. H.; Fessenden, R. W. *J. Phys. Chem.* **1971**, *75*, 1186−1201.
(198) Sealy, R. C.; Harman, L.; West, P. R.; Mason, R. P. *J. Am. Chem. Soc.* **1985**, *107*, 3401−3406.
(199) Schwarz, H. A.; Dodson, R. W. *J. Phys. Chem.* **1984**, *88*, 3643−3647.
(200) Lilie, J.; Beck, G.; Henglein, A. *Ber. Bunsen-Ges. Phys. Chem.* **1971**, *75*, 458−465.
(201) Sarala, R.; Islam, M. A.; Rabin, S. B.; Stanbury, D. M. *Inorg. Chem.* **1990**, *29*, 1133−1142.
(202) Das, T. N.; Huie, R. E.; Neta, P. *J. Phys. Chem. A* **1999**, *103*, 3581−3588.
(203) Huie, R. E.; Clifton, C. L.; Neta, P. *Radiat. Phys. Chem.* **1991**, *38*, 477−481.
(204) Schwarz, H. A.; Bielski, B. H. J. *J. Phys. Chem.* **1986**, *90*, 1445−1448.
(205) Ram, M. S.; Stanbury, D. M. *J. Phys. Chem.* **1986**, *90*, 3691−3696.
(206) Ilan, Y. A.; Czapski, G.; Meisel, D. *Biochim. Biophys. Acta* **1976**, *430*, 209−224. *100*, 9892−9899.